

**Systematic Investigations of the  
Anionic Ring Opening Polymerization of Polyglycerol and  
Synthesis of Functional Polyglycerol Sulfates**

DISSERTATION

zur Erlangung des akademischen Grades des  
Doktors der Naturwissenschaften (Dr. rer. nat.)

eingereicht im Fachbereich Biologie, Chemie, Pharmazie  
der Freien Universität Berlin

vorgelegt von

**Florian Paulus, M. Sc.**

aus Deckenpfromm

März 2014

Diese Arbeit wurde unter Anleitung von Prof. Dr. Rainer Haag im Zeitraum von November 2009 bis März 2014 am Institut für Chemie und Biochemie der Freien Universität Berlin angefertigt.

1. Gutachter: Prof. Dr. Rainer Haag
2. Gutachter: PD Dr. Kai Licha

Disputation am 06.05.2014



*Meinen Eltern*



## **Acknowledgements**

First of all I would like to thank Prof. Dr. Rainer Haag for the opportunity to do my PhD thesis in his group and for the scientific support during the last four years. Further, I would like to thank PD Dr. Kai Licha for taking over the second expertise and the helpful discussions we regularly had.

All members of the Haag group are thanked for the support, collaborations, scientific discussions, and the great time we spent together over the last years. The Tzschucke group is gratefully acknowledged for the shelter in their laboratories. I want to thank the whole group for the scientific discussions and the nice time together. The Calderon group and the Seiffert group is thanked for scientific discussions throughout my PhD.

Very special thanks to the group of Prof. Dr. Jayachandran Kizhakkedathu and Prof. Donald Brooks for the scientific support, the collaborations and the great time during my stay as visiting scientist at the Centre of Blood Research, UBC, Canada.

Dr. Dirk Steinhilber is highly acknowledged for the scientific support and the great time during my entire PhD. He helped me to keep my Swabian language.

Cathleen Schlesener is gratefully acknowledged for the uncountable GPC measurements which were irreplaceable for this work.

Very special thanks to all my cooperation partners. Especially PD Dr. Kai Licha, PD Dr. Pia Welker, Sylvia Kern, Nicole Wegner, Ingo Steinke and Dorothea Mangoldt from the mivenion GmbH, Dr. Jens Dervedde, Dr. Sebastian Riese and Ronny Schulze from the Charité Berlin, Dr. Stefanie Wedepohl from the Calderon group of the FU Berlin, Dr. Harald Depner from the Biology Department of the FU Berlin, Dr. Maximilian Weiss and Prof. Dr. Christof Schütte from the Department of Mathematics and Computer Sciences of the FU Berlin, Dr. Maximilian Zieringer from the Harvard School of Engineering and Applied Sciences, Cambridge, Dr. Anatoly Nikitin from the Institute on Laser and Information Technologies in Moscow, Dr. Helmut Schlaad and Marlies Graewert from the MPI of Colloids and Interfaces in Potsdam.

Further thanks to my former and present lab colleagues, Dr. Dirk Steinhilber, Dr. Rahul Tyagi, Dr. Wei Chen, Dr. Michal Andrä, Sasa Duric, Sabrina Nowak, Ralf Albrecht, Anja Sokolowski, Fanni Daruni Sypaseuth, Swantje Wiebalk, Sina Zucker, Emma Svensson, Laura Vossen, Cindy Glor, Mathias Dimde, Daniel Stöbener, Era Kapourani for the nice and relaxed working atmosphere.

The analytical department of the Institute of Chemistry and Biochemistry is acknowledged for numerous NMR, MS and elementary analysis measurements. The material store is thanked for all the “5-past-4-orders.” Michael Mühlbrandt is thanked for repairing a lot of electronic equipment. The workshop and the glass factory are acknowledged for manufacturing special equipment and repairing all the broken glass ware.

Special thanks to all my colleagues with whom I regularly enjoyed lunch and coffee, the “11:15”, the “11:30”, the “12:15”, the JKI group and the special “W\*\*\*\*\*n Lunch” group for the lively private and scientific discussions.

I am grateful to PD Kai Licha, Dr. Pamela Winchester, Dr. Dirk Steinhilber, Dr. Jens Dervedde, Dr. Juliane Keilitz, Dr. Harald Depner, Dr. Emanuel Fleige, and Daniel Stöbener for proof reading of numerous publications and manuscript drafts, including this thesis.

I would like to thank all my friends who accompanied me throughout my whole PhD, especially, for spending several nice hours with me that I greatly enjoyed.

A very special thanks to my family, especially my parents for the private and financial support during my whole education. You have always believed in me and tried to keep up my motivation.

Finally, I am eternally grateful to my beloved fiancée Daniela. You were always there for me, you lifted me up when I was frustrated, you helped me through bad times and enjoyed the good times with me. I love you with all my heart.





## Table of Contents

1	Introduction .....	1
1.1	Drug Delivery Systems in Nanomedicine .....	1
1.1.1	General Aspects of the Application of Polymeric Drug Delivery Systems .....	1
1.1.2	Polyglycerol Based Drug Delivery Systems .....	5
1.2	Polyanions as Anti-Inflammatory Agents .....	12
1.2.1	The Response of the Immune System .....	12
1.2.2	The Inflammation Cascade.....	12
1.2.3	Structure-Activity Relationship of Polyanionic Inhibitors.....	15
1.2.3.1	Characterization of the Anti-Inflammatory Properties.....	15
1.2.3.2	Dendritic Polyglycerol Sulfates as Anti-Inflammatory Agent .....	16
1.3	Synthesis of Dendritic Polymers .....	23
1.3.1	Polymer Architectures .....	23
1.3.2	Hyperbranched Polymers .....	24
1.3.3	Historical Development of Hyperbranched Polyglycerols.....	28
1.3.4	State-of-the-Art in Polyglycerol Synthesis.....	30
1.3.5	Basic Principles for Polymerization Mechanisms and Kinetics.....	33
2	Scientific Goal.....	35
3	Publications and Manuscripts.....	37
3.1	Estimating Kinetic Parameters for the Spontaneous Polymerization of Glycidol at Elevated Temperatures .....	37
3.2	Anionic Ring-Opening Polymerization Simulations for Hyperbranched Polyglycerols with Defined Molecular Weights .....	50
3.3	The Effect of Polyglycerol Sulfate Branching On Inflammatory Processes .....	68
3.4	Structure Related Transport Properties and Cellular Uptake of Hyperbranched Polyglycerol Sulfates with Hydrophobic Cores .....	93
4	Summary and Conclusion .....	114
5	Outlook.....	116

6	Zusammenfassung .....	117
7	References .....	119
8	Patent Applications, Publications and Conference Contributions.....	126
8.1	Patent Applications.....	126
8.2	Publications .....	126
8.3	Conference Contributions.....	127
9	Curriculum Vitae.....	129

## List of Abbreviations

A2780	Human ovarian carcinoma cell line
A549	Human lung carcinoma epithelial cell line
ADME	Administration–distribution–metabolization–excretion
AuNP	Gold nanoparticle
BF <sub>3</sub> ·EtO <sub>2</sub>	Boron trifluoride diethyl etherate
bisMPA	2,2-Bis(hydroxymethyl)propionic acid
CAC	Critical aggregation concentration
CAM	Cell adhesion molecule
CCA	Classical complement activity
CLSM	Confocal laser scanning microscopy
CMC	Critical micelle concentration
CME	Clathrin-mediated endocytosis
CMS	Core-multishell
CR	Complement regulatory domains
CRD	Carbohydrate recognition domain
CS	Core-shell
DB	Degree of branching
DDS	Drug delivery system
DF	Degree of functionalization
DI	Dispersity index
DLS	Dynamic light scattering
DMM	Double monomer methodology
dPG	Dendritic polyglycerol
dPGP	Dendritic polyglycerol phosphate sodium salt
dPGS	Dendritic polyglycerol sulfate
DS	Degree of sulfation
EEGE	Ethoxyethyl glycidol ether
EGF	Epidermal growth factor
EPR	Enhanced Permeability and Retention
ESL	E-selectin ligand
FACS	Fluorescence activated cell scanning
GMA	Glycidyl methacrylate
HPF <sub>6</sub> ·OEt <sub>2</sub>	Hexafluorophosphoric acid diethyl etherate

ICAM	Intercellular adhesion molecule
ICC	Indocarbocyanine
KOH	Potassium hydroxide
KO <i>t</i> Bu	Potassium <i>tert</i> -butoxide
LMWH	Low molecular weight heparin
MAdCAM	Mucosal addressin cell adhesion molecule
MMWH	Medium molecular weight heparin
$M_n$	Number average molecular weight
mPEG	Poly(ethylene glycol) monomethyl ether
$M_w$	Weight average molecular weight
MW	Molecular weight
MWD	Molecular weight distribution
NaOMe	Sodium methoxide
PAA	Poly(acryl amide)
PAMAM	Poly(amido amine)
PDEAEMA	Poly(diethylaminoethylmethacrylate)
PDMS	Poly( <i>N</i> -methyldietheneamine sebacate)
PE	Polyethylene
PECAM	Platelet/endothelial cell adhesion molecule
PEG	Poly(ethylene glycol)
PEI	Poly(ethylene imine)
PEO	Poly(ethylene oxide)
PLA	Poly(lactide)
PLGA	Poly(lactide- <i>co</i> -glycolide)
PNIPAm	Poly( <i>N</i> -isopropyl acrylamide)
PTT	Partial thromboplastin time
PSGL	P-selectin glycoprotein ligand
PTP	Proton transfer polymerization
PVP	Poly( <i>N</i> -vinylpyrrolidone)
QGP-1	Epithelial human pancreatic cancer cell line
ROMBP	Ring-opening multibranching polymerization
SCROP	Self-condensing ring-opening polymerization
SCVP	Self-condensing vinyl polymerization
SiaLe <sup>a</sup>	sialyl Lewis a

SiaLe <sup>x</sup>	sialyl Lewis x
SMA	Slow monomer addition
SMM	Single monomer methodology
SnCl <sub>2</sub>	Tin(II) chloride
SO <sub>3</sub> -Pyr	Sulfur trioxide pyridine complex
SPR	Surface plasmon resonance
TC	Transport capacity
TEA	Triethyl amine
UFH	Unfractionated heparin
VCAM	Vascular cell adhesion molecule

## 1 Introduction

### 1.1 Drug Delivery Systems in Nanomedicine

#### 1.1.1 General Aspects of the Application of Polymeric Drug Delivery Systems

At the end of the 20<sup>th</sup> century a very specialized field in biomedicine emerged, referred to as polymer therapeutics.<sup>[1]</sup> Polymer therapeutics are generally defined as nano-sized medicines which comprise polymeric drugs, polymer-drug conjugates, polymer-protein conjugates, polymeric micelles, and polymeric non-viral vectors for gene delivery.<sup>[2]</sup> Although the general concept was already presented almost 30 years before, the introduction of dendritic polymeric scaffolds opened new opportunities.<sup>[3]</sup> Due to their unique properties, e.g., high functionality and a (partially) spherical architecture, dendritic polymers are applied in various applications nowadays and will be discussed in more detail in Chapter 1.3.1. In the field of drug delivery systems (DDS), the application of dendritic macromolecules was extensively studied for several decades.<sup>[4]</sup>

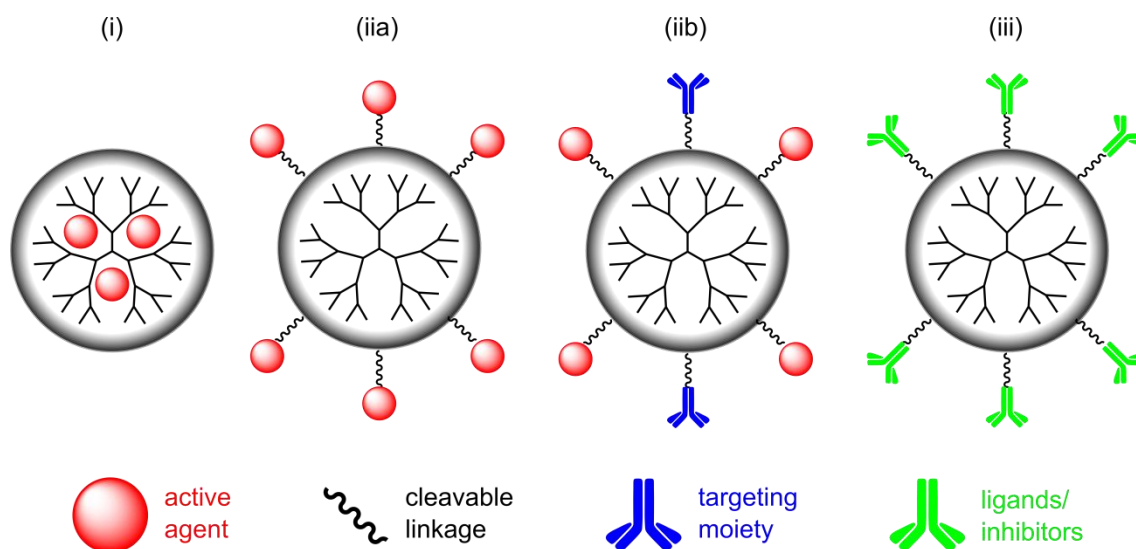


**Figure 1:** General concepts for DDS systems based on dendritic scaffolds: (i) the active agent is supramolecularly encapsulated in the host molecule, (iia) the active agent is coupled to the polymer scaffold without or (iib) with a targeting moiety, (iii) the ligand/inhibitor is multivalently presented on the polymer surface and the functionalized polymer scaffold is the active agent. Figure adapted from literature.<sup>[3b]</sup>

In general, DDS are based on three different concepts (see Figure 1): (i) the active agent is supramolecularly encapsulated into the dendritic scaffold or its aggregates, (ii) the active agent is covalently attached to the scaffold via a cleavable linker (iia) without or

(iib) with a targeting moiety, and (iii) the terminal groups of the dendritic scaffold are functionalized with pharmacologically active groups, e.g., sulfates.<sup>[3b]</sup> The latter concept, well-known as the Ringsdorf model for polymer therapeutics, will be discussed in Chapter 1.2. The concept of utilizing these polymeric DDS is based on a simple principle: in nanomedical applications, pharmaceutically active agents need to be administered to the human body via different routes and accumulated in the requested region to obtain a therapeutic effect.<sup>[5]</sup> This delivery step already implements the first hurdle, as active agents are usually lipophilic and of low-molecular weight with hardly predictable pharmacokinetics/-dynamics and absorption-distribution-metabolization-excretion (ADME) behavior.<sup>[4a, 6]</sup> In consequence, small molecular drugs with poor water solubility are absorbed extremely inefficient. Regarding the fast renal excretion of small molecules below the threshold of  $45\ 000\ \text{g mol}^{-1}$  or  $4\text{-}9\ \text{nm}$ ,<sup>[7]</sup> the blood circulation and retention time is very small and continuous treatment with high dosage are necessary to stay within the therapeutic window. Therapies with high and repeating dosage can cause severe side effects (as discussed for heparin in Chapter 1.2.3.2.)<sup>[8]</sup>

Both major disadvantages of toxicity and bioavailability can be addressed by DDS for several reasons. The utilization of macromolecular carriers significantly enhances the water solubility, reduces renal excretion, and therefore increases the blood circulation and bioavailability in the blood stream, which in turn reduces the number of treatment sessions and dosage.<sup>[9]</sup> A low immunogenicity and high biocompatibility, i.e., reduced blood interaction and complement activation, are also attributed as “stealth/shielding” properties of certain polymers used for DDS.<sup>[10]</sup> Especially poly(ethylene glycol) (PEG, PEO) is well known for its extraordinary shielding properties.<sup>[11]</sup> The stealth properties of PEG can be amplified upon multivalent presentation on a multifunctional scaffold, e.g., dendritic polymers, liposomes, or polymersomes.<sup>[3a, 4a, 12]</sup>

In addition to the above mentioned bioavailability issues of polymeric DDS, the particle size and molecular weight play a crucial role in the absorption, distribution, and metabolization of the ADME pathway. In case of tumor targeting the optimal DDS size was determined to  $10\text{--}300\ \text{nm}$  depending on the investigated tumor tissue with pore cut offs around  $380\text{--}780\ \text{nm}$ .<sup>[13]</sup> A polymeric DDS with this specifications and consequently prolonged blood circulation time is able to benefit from the enhanced permeability and retention (EPR) effect (see Figure 2), which is considered as a passive targeting mechanism.<sup>[14]</sup>

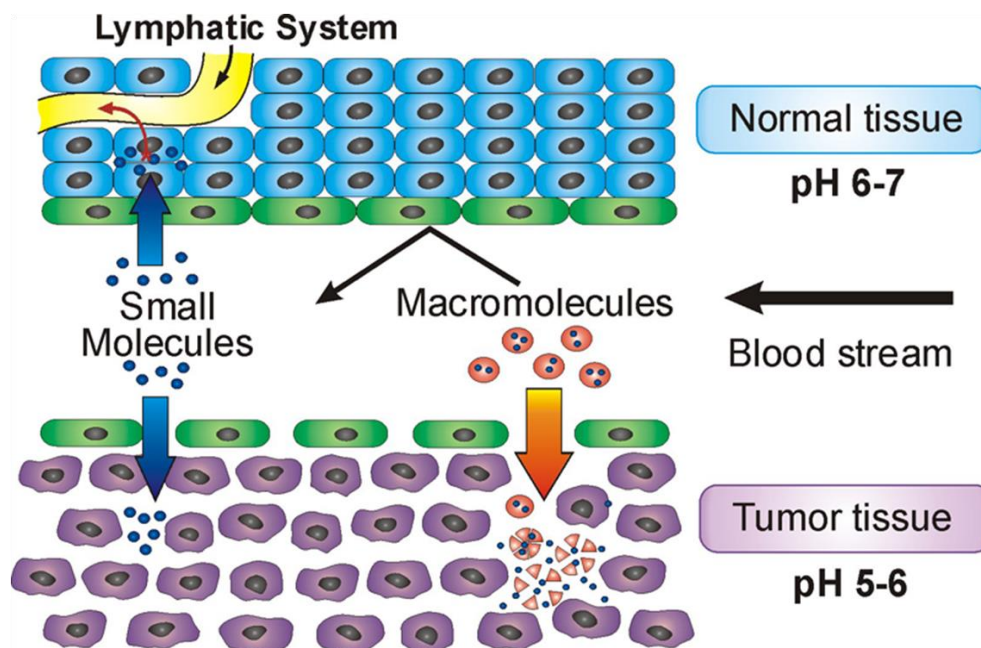


**Figure 2:** Schematic presentation of the enhanced vascular permeability and retention (EPR effect) of small molecules and macromolecules in healthy and inflamed/tumor tissue and the possible clearance by the lymphatic system. Figure was reprinted from literature.<sup>[3a]</sup>

The EPR effect is attributed to the porous and leaky tissue structure of tumors and inflamed areas. Whereas healthy tissue is protected by a compact endothelial cell layer, the endothelium on the tumor is porous and disrupted, because of the unnaturally fast growth of the tumor tissue. While small molecules can penetrate unselectively into healthy and diseased tissue, where they are rapidly cleared by the lymphatic system, macromolecules on the other hand, are preferentially accumulated by the fenestrated tissue of tumors and sites of inflammation.

In order to induce a therapeutic effect, the DDS has to enter the cell by crossing the cell membrane after extravasation into the tumor tissue. This cellular compartmentalization is based on a multistep pathway (see Figure 3).<sup>[15]</sup> The internalization properties of any DDS can be related to its physicochemical properties, e.g., size, shape, charge, surface chemistry, surface topology, and mechanical properties.<sup>[16]</sup> The most extensively studied uptake mechanism is the clathrin-mediated endocytosis (CME) pathway of, e.g., nutrients or viruses, with particle sizes below 300 nm.<sup>[17]</sup> A very special, but rather unexplored way of uptake within this region is the calveolae-mediated endocytosis route for particles sizes from approx. 50 to 80 nm. Several viruses and cholera toxins are known to enter cells via this pathway.<sup>[18]</sup>



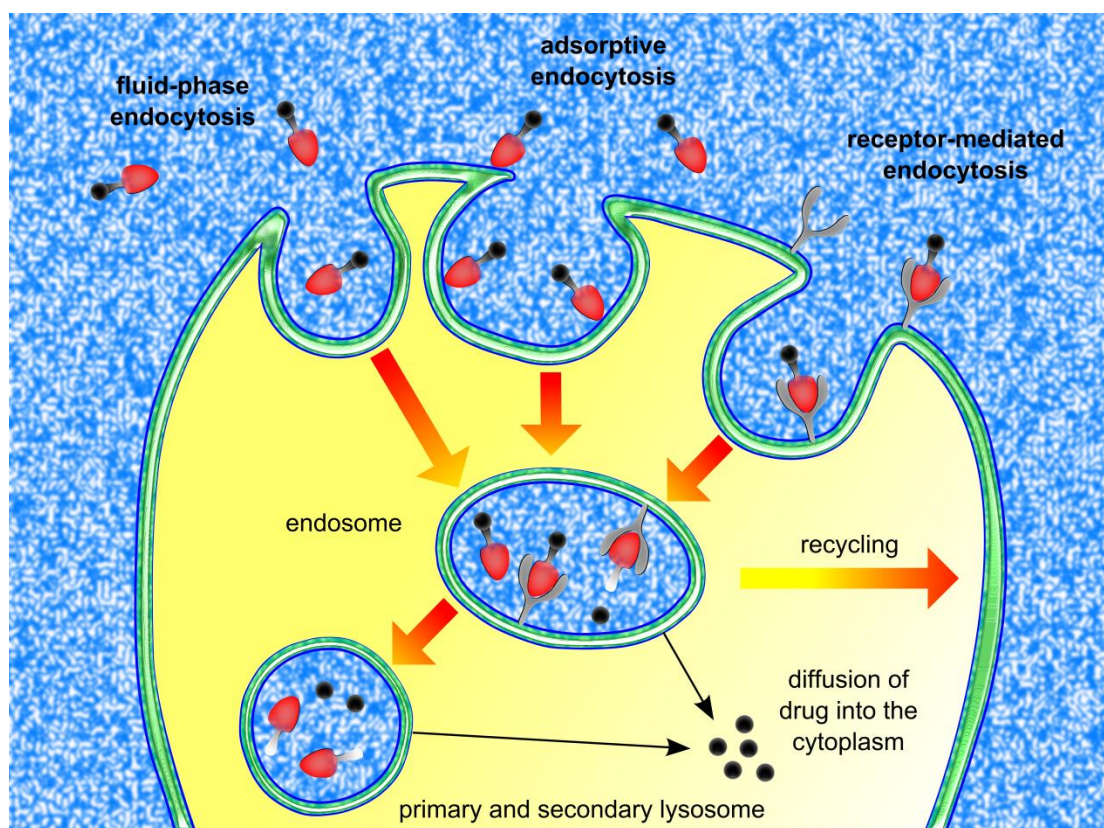


**Figure 3:** General schematic pathway for the endocytosis of macromolecules by fluid-phase, adsorptive, and receptor mediated endocytosis, with respect to a passive or active targeting strategy. Figure adapted from literature.<sup>[3a]</sup>

A systematic study regarding the surface functionality of poly(amido amine) (PAMAM) dendrimers showed that only negatively charged particles enter the cell via the calveolae-mediated pathway.<sup>[19]</sup> Both neutral and positively charged polymers were endocytosed via non-clathrin, non-calveolae-mediated pathways mainly driven by electrostatic and non-specific interactions. The consecutive important step to successfully deliver an active agent is the endosomal/lysosomal escape. The “proton sponge” hypothesis was introduced for the first time to describe this internalization mechanism for poly(ethylene imine) (PEI) and other polycations.<sup>[20]</sup> Although this part of the endocytosis is heavily debated on, it is crucial for the delivery to the target in the cytoplasm and so far the most accepted mechanism.<sup>[21]</sup> During the transfer from the early to the late endosome and finally fusion with the lysosome for degradation, a rapid drop from the physiological pH to approx. 5 occurs. According to the “proton sponge” effect theory different groups on the polymer, e.g., amine groups for PEI can absorb protons and consequently reduce the

drop in pH.<sup>[22]</sup> Because of an osmotic imbalance, the influx of protons and chloride ions is enhanced which induces osmotic swelling and in an ideal case, rupturing of the endosome. This endosomal/lysosomal escape mechanism is generally adopted to describe the endocytosis of polyplexes formed of polycations and nucleic acids.<sup>[23]</sup> The first step in endocytosis is regulated by the cellular membrane, which determines the efficacy of the uptake. Depending on the physicochemical properties of the DDS mentioned above, the endocytosis proceeds via fluid-phase, adsorption, or receptor-mediated interactions. However, the properties which enhance the uptake can also have an opposing effect, e.g., when applying highly charged or large particles above 200-300 nm. The following chapters discuss supramolecular nanocarrier systems based on polyglycerol scaffolds as potent drug delivery systems in more detail.

### 1.1.2 Polyglycerol Based Drug Delivery Systems

As a result of their spherical architecture, dendritic molecules are able to host guest molecules, e.g., drugs, dyes, and other pharmaceutically active molecules in their cavities.<sup>[24]</sup> The guest molecules are physically stabilized by electrostatic interactions, hydrogen bonding, dipole-dipole, and hydrophobic interactions. Meijer and coworkers studied the so-called “dendritic box” by synthesizing poly(propylene imine) (PPI) dendrimers for supramolecular encapsulation of hydrophobic guests.<sup>[25]</sup> The host properties were achieved by chemical surface modification of the functional groups, which resulted in a dense shell surrounding the dendrimer. Although the synthesized polymer was not water soluble, the general concept of core-shell (CS) architectures inspired the chemical society to further investigate similar structures, consisting of a hydrophobic core and a polar dense shell.

Among other hyperbranched polymers (discussed in Chapter 1.3.2), dendritic polyglycerol (dPG) represents an ideal, biocompatible scaffold to synthesize CS architectures.<sup>[26]</sup> Haag and coworkers followed a post-synthetic functionalization strategy of the inner hydroxyl groups of the dPG, to introduce hydrophobic moieties into the interior scaffold.<sup>[27]</sup> Upon acetal protection of the peripheral hydroxyl groups, derivatized biphenylmethyl ether groups were introduced to a dPG with  $5\,000\text{ g mol}^{-1}$  exclusively into the core. With a maximum degree of functionalization (DF) of 44%, the amphiphilic architectures were able to transport up to 5.7 and 5.2 mg of Pyrene and Nimodipine per gram polymer, respectively. Any higher DF yielded water insoluble CS architectures. A similar study investigated the transport capacities (TC) of dPGs with internal biphenyl

ester, perfluorinated thiol ether, and perfluorinated ester groups.<sup>[28]</sup> The TC of guest molecules Pyrene, Nile Red, and Nimodipine were investigated. In case of Pyrene, the perfluorinated thiol esters yielded the highest TC. Nile Red was equally well solubilized by highly functionalized biphenyl ester and perfluorinated cores with a TC of up to 20.3 mg g<sup>-1</sup>. For Nimodipine, a TC of 18.9 mg g<sup>-1</sup> was achieved for the biphenyl ester derivatized core. Haag and coworkers further elaborated the structure-transport relationship of biphenyl-derivatized, PEGylated, core-shell architectures according to the same strategy utilizing a post-functionalization methodology (see Figure 4).<sup>[29]</sup>

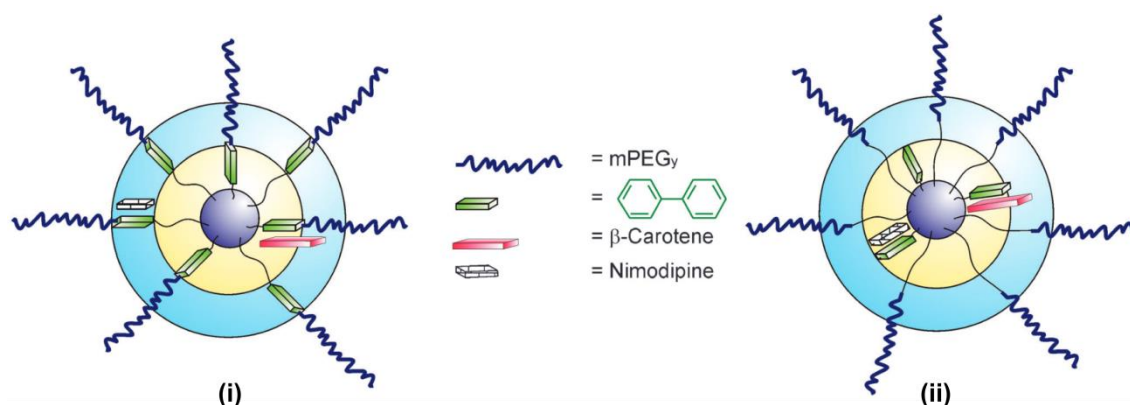


**Figure 4:** Representation of CS architectures with (i) randomly distributed and (ii) exclusively core-derivatized hydrophobic moieties. In addition, the figure presents the encapsulation properties of non-polar guest molecules. Figure was reprinted from literature.<sup>[29]</sup>

Encapsulation studies with the guest molecules Nimodipine, Rose Bengal, Congo Red, and  $\beta$ -Carotene showed that a defined CS architecture with a biphenyl ester derivatized dPG core and a dense PEG shell is able to transport guest molecules more efficiently compared to randomly distributed hydrophobic moieties within the scaffold.

An easier strategy for synthesizing CS architectures is the incorporation of a hydrophobic core as initiator. Steinhilber et al. utilized a grafting-from approach to attach dPG to a calix[8]arene core.<sup>[30]</sup> The macromonomers with  $M_n = 6\,500\text{ g mol}^{-1}$  were able to stabilize an indocarbocyanine (ICC) dye and reduced the photobleaching effect. The photobleaching of the ICC dye was even further reduced, when the PG-based macromonomers were embedded in a microgel. The building blocks were functionalized with approx. 5% acrylic groups to perform the gelation of the precursor. This approach perfectly demonstrated the diversity of the dPG toolbox system (described in Chapter 1.3.3).

Brooks and coworkers applied a different multistep strategy to synthesize a hydrophobically derivatized dPG.<sup>[31]</sup> The hydrophilic dPG core was functionalized with the aliphatic monomer 1,2-epoxyoctadecane, followed by PEG monomethyl ether (mPEG). Although the hydrophobic compartments are not exclusively attached to peripheral hydroxyl groups of the core, it can be described as an inner hydrophobic layer. This type of core-shell-type systems are considered as unimolecular micelles. In contrast to (self-assembled) micelles, these carriers are stable upon dilution. Newkome and coworkers coined the concept of unimolecular micelles and introduced it to the chemical society in 1991.<sup>[32]</sup> Based on the research of Ringsdorf on the basic principles of self-organization,<sup>[33]</sup> Newkome and coworkers developed a unimolecular, symmetrical, four-directional hydrocarbon cascade polymer including peripheral carboxylic acid functionalities. This architecture was able to transport hydrophobic guest molecules in the lipophilic core. Since then, many studies on different CS architectures showed the diversity of this concept. Stevelmans and coworkers reported an inverted unimolecular dendritic micelle based on PEI dendrimers functionalized with an aliphatic palmitoyl shell.<sup>[34]</sup> However, PEGylated systems were predominantly investigated because of their stealth properties and the solubility of PEG in a wide range of organic solvents as well as water. Fully PEGylated PAMAM dendrimers were utilized as hosts for the anticancer drugs doxorubicin and methotrexate.<sup>[35]</sup> Partially PEGylated PAMAM dendrimers (DF < 10%) of different generations showed very high DNA transfection capacities with low cytotoxicity.<sup>[36]</sup> Haag and coworkers recently published a unimolecular transporter based on a CS architecture comprising a high-molecular weight branched polyethylene (PE) core with a grafted dPG shell.<sup>[37]</sup> The PE core was synthesized by a chain-walking polymerization which allowed the control of the topology of the PE core regarding the degree of branching (DB) and the molecular weight by variation of the ethylene atmosphere.<sup>[38]</sup>

Another very promising universal nanocarrier is based on a core-multishell (CMS) architecture.<sup>[39]</sup> Aliphatic building blocks C<sub>6</sub>, C<sub>8</sub>, and C<sub>18</sub> dicarboxylic acids were mono-functionalized with different PEGs (6, 10, 14 average glycol repeating units), as presented in Figure 5. The so-called double shell was covalently coupled to the peripheral amine groups of PEI cores with 3 600 and 10 500 g mol<sup>-1</sup> with an average DF between 70-100%. The synthesized CMS architectures were able to transport different hydrophobic and hydrophilic guests in organic and aqueous media. These CMS architectures were soluble in a variety of solvents ranging from water to toluene and were described as “chemical chameleons”.

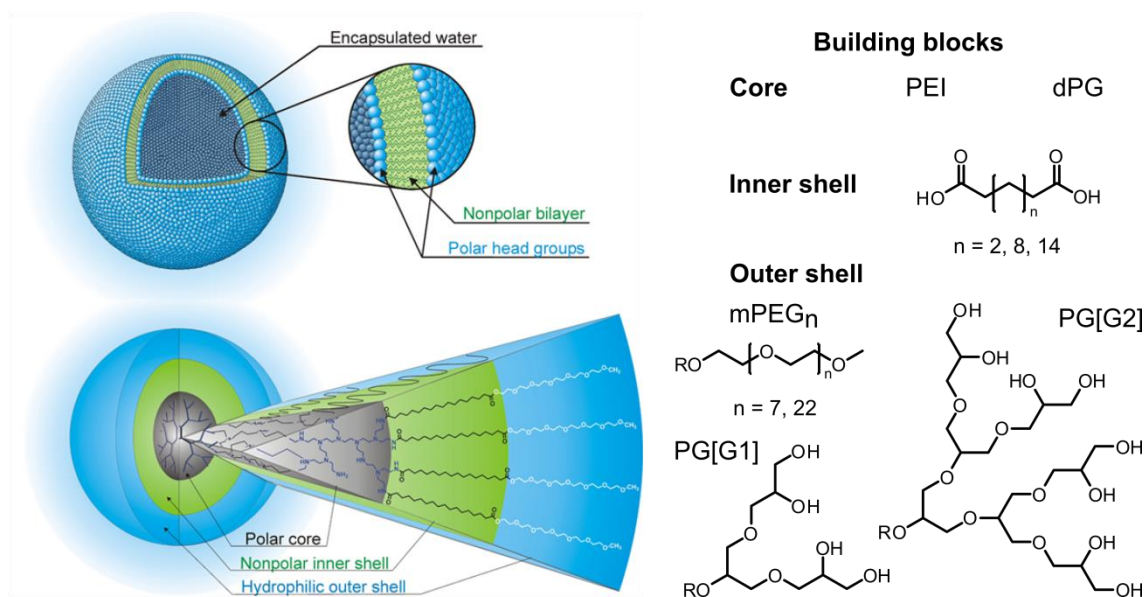


**Figure 5:** CMS architectures based on PEI or dPG cores, an aliphatic non-polar inner shell, and a hydrophilic outer shell. Different dicarboxylic acids have been investigated as well as different linear and dendronized water-soluble outer shells. CMS architectures mimic natural (bilayer) vesicles. Figure adapted from literature.<sup>[40]</sup>

The CMS was designed in analogy to natural liposomes on a unimolecular basis.<sup>[3a]</sup> The CMS mimics self-associated bilayer vesicles with the dPG core as the aqueous interior; the aliphatic chain as the hydrophobic bilayer; and the PEG chain as the aqueous surrounding medium, with an additional stealth property.<sup>[41]</sup> After the potentially toxic PEI core was exchanged with a biocompatible dPG core, these promising nanocarriers were further investigated in vitro regarding the localization of the encapsulated molecules in one of the outer shells,<sup>[42]</sup> their skin penetration properties,<sup>[43]</sup> or the TC upon exchange of the outer PEG shell with PG dendrons.<sup>[40b]</sup>

As discussed before, unimolecular nanocarriers are stable upon dilution. However, supramolecular assemblies which form at different concentrations can also be beneficial for certain applications.<sup>[44]</sup> Amphiphilic polymers contain at least one hydrophobic and one hydrophilic building block of a certain length.<sup>[33]</sup> Various polymers can be applied as building block, e.g., poly(*N*-vinylpyrrolidone) (PVP),<sup>[45]</sup> poly(*N*-isopropyl acrylamide) (PNIPAm),<sup>[46]</sup> and PEG for the hydrophilic block. Common polymers used for the hydrophobic block are poly(lactide) (PLA)<sup>[47]</sup> and poly(lactide-*co*-glycolide) (PLGA), whereas the latter polymer is biodegradable.<sup>[48]</sup> Depending on the size and structure of each

individual block, the amphiphiles assemble forming different aggregated architectures, e.g., bilayers, spherical micelles, or rod-like micelles. The assembly process can be initiated by different stimuli. Below the critical micelle concentration (CMC) or, in case of polymers, the critical aggregation concentration (CAC), the process can only start upon addition of guest molecules. Depending on the polarity of the continuous phase and the guest, the individual amphiphiles form normal or inverse host micelles. Above the CMC, the amphiphiles spontaneously self-assemble to the described systems. Non-ionic dendritic glycerol amphiphiles were investigated for their excellent solubilization of a poorly water-soluble anticancer drug.<sup>[49]</sup> The drug molecule was encapsulated in defined micelles depending on the structure of the hydrophobic aliphatic tail and its functionalization with a bi-aromatic structure. In a consecutive study, the aggregation behavior of amphiphiles, containing different generations of glycerol dendrons, with respect to the hydrophobicity of the guest molecules was investigated.<sup>[50]</sup> The amphiphiles showed different aggregation behavior dependent on the size of the dendrons, the linkage to the hydrophobic tail and the hydrophobicity of the aromatic model guest. Gupta et al. used an enzymatic approach to synthesize biodegradable diblock polymers based on PG dendrons of generation 1 and 2 by utilizing Novozym-435 as biocatalyst.<sup>[51]</sup> The different multi-amphiphiles were able to encapsulate hydrophobic guests like Pyrene and 1-anilinonaphthalene-8-sulfonic acid within the hydrophobic core of the micelles. Although self-assembled polymeric micelles are fairly stable above the CAC, the supramolecular interactions are sensitive, e.g., towards pH, salt concentration or temperature.

The second principle of DDS is based on the covalent attachment of an active agent onto the polymer scaffold via a cleavable linker (see Figure 6).<sup>[1a, 4b]</sup> A variety of functional groups of organic chemistry were investigated as tunable cleavable moieties.<sup>[52]</sup> pH responsive systems are often based on acetal, imine, hydrazone, or hydrazide bonds, depending on the required pH for the cleavage for example of acrylate systems like poly(acrylamide) (PAA), poly(diethylaminoethyl methacrylate) (PDEAEMA), or glycerol-based systems.<sup>[53]</sup> Calderón and coworkers were able to transport doxorubicin in an ovarian xenograft tumor model by utilizing a dPG core with the drug covalently attached over an acid-sensitive hydrazine linkage and post PEGylation of the polymer conjugate. Wang and coworkers synthesized a biodegradable cationic amphiphilic copolymer with cholesterol side chains for the co-delivery of drugs and DNA into mouse and human breast cancer models.<sup>[54]</sup> In various studies disulfide bonds were utilized as reductively cleavable systems based on peptides, proteins, or liposomes.<sup>[55]</sup> Naturally occurring enzymes were



investigated to trigger the release of a pharmacologically active agent. The enzymatic cathepsin B cleavable derivative of the anticancer drug doxorubicin was coupled to a PG core which was functionalized with 20% amine groups.<sup>[56]</sup> The polymer conjugates showed high loading ratios and the doxorubicin was efficiently released in the presence of cathepsin B. UV-responsive DDS were reported to efficiently transport and release DNA upon irradiation, based on poly(*N*-methyldietheneamine sebacate) (PDMS), and cationic cleavable gold nanoparticles (PC-AuNP).<sup>[57]</sup>

In general, the application of DDS and especially polymer drug conjugates according to the second strategy described above is mainly limited by the solubility of the conjugate. As active agents are generally hydrophobic, the loading of the formerly soluble polymer backbone decreases the solubility and its usability. In contrast, the Ringsdorf model offers an excellent and facile strategy to solve this solubility limitation, because the polymer scaffold has a large number of functional groups which can be functionalized with additional solubilizing groups, if required (see Figure 6). Furthermore, a certain ratio of the functional groups can be functionalized with active targeting moieties, e.g., antibodies, saccharides, or ligands for pharmacologically interesting receptors.<sup>[58]</sup>

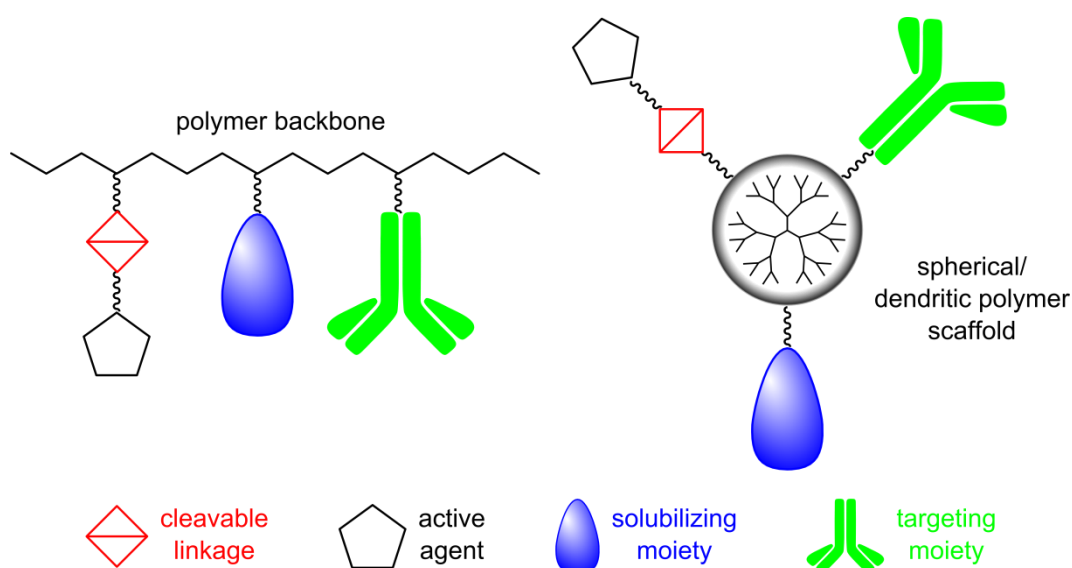


**Figure 6:** Ringsdorf model for drug delivery systems with the basic functionalities: the active agent is attached to the polymeric scaffold via a cleavable linkage. The multifunctional polymer can be functionalized with solubilizing groups and targeting moieties, depending on its nature and the desired application. Figure adapted from literature.<sup>[4a]</sup>

In addition to the enhanced bioavailability deriving from the large molecular weight of the polymeric scaffold and the resulting EPR effect, the DDS can actively approach its

target, e.g., tumors with an overexpressed receptor. The strategy of active targeting resulted in a third concept for DDS, which is based on the multivalent presentation of targeting and/or solubilizing ligands on the polymer periphery to turn the polymer into a pharmacologically active agent itself.<sup>[59]</sup> This concept will be further discussed in the following Chapter 1.2, including its impact on the immune system and inflammatory processes.



## 1.2 Polyanions as Anti-Inflammatory Agents

### 1.2.1 The Response of the Immune System

In general, an inflammation is the response of the innate and adaptive immune system to external pathogens, viruses, or other harmful stimuli. Any inflammatory process can be classified as either an acute or chronic condition. In an acute setting the inflammatory activity is induced and mediated, e.g., by mast cells, macrophages, or neutrophil cells,<sup>[60]</sup> which are able to defend pathogens directly and release a variety of pro-inflammatory signaling factors to attract further cells. Typical signs of inflamed tissue are warming, redness, and itchiness. Although acute inflammation can cause severe pain, and in some cases loss of function, it also indicates the initiation of the healing process.<sup>[61]</sup> The acute response starts rapidly, but its symptoms only last for several days. Well known examples are acute bronchitis, allergic reactions, or a sore throat. However, if the healing process is disturbed, ongoing tissue destruction might occur or abscess formation develops, which is local accumulation of sanies (neutrophils). If not treated accordingly, an acute inflammation can also turn to a chronic disease. Prolonged or chronic inflammation, as occurring in asthma, tuberculosis, or rheumatoid arthritis, can last for an unpredictable period of time. Chronic inflammation is usually related to a defect within the body which cannot be eliminated immediately. In some cases, an autoimmune response is the reason, where the immune system mistakenly attacks a self-antigen. In this case, tissue healing and destruction occurs concurrently due to autoantibodies and auto-reactive T-cells

In any inflammatory disease, the recruitment of circulating leukocytes from the blood stream represents the crucial step.<sup>[62]</sup> In order to design anti-inflammatory agents to dampen exaggerated immune response, it is important to understand the exact inflammatory cascade. Therefore, the following section focuses on the mechanism of the inflammation process including its most important steps.

### 1.2.2 The Inflammation Cascade

The recruitment of leukocytes from the blood stream into the inflamed tissue is the first key step of the inflammation cascade (Figure 7). The interaction between the leukocytes and endothelia is mediated by cell adhesion molecules (CAMs) presented on the leukocytes, the vascular endothelium, and on platelets. Among others, CAMs comprise L-selectins, expressed on the leukocyte, P-selectins presented on platelets and the endothelium, vascular cell adhesion molecule-1 (VCAM), intercellular adhesion molecule-

1 (ICAM), and mucosal addressin cell adhesion molecule-1 (MAdCAM-1) which interact with carbohydrate ligands presented on the cell surface. The up-regulation, activation, or the release of intracellular CAMs is triggered by pro-inflammatory stimuli, e.g., cytokines responsible to initiate the inflammatory cascade of leukocyte recruitment.

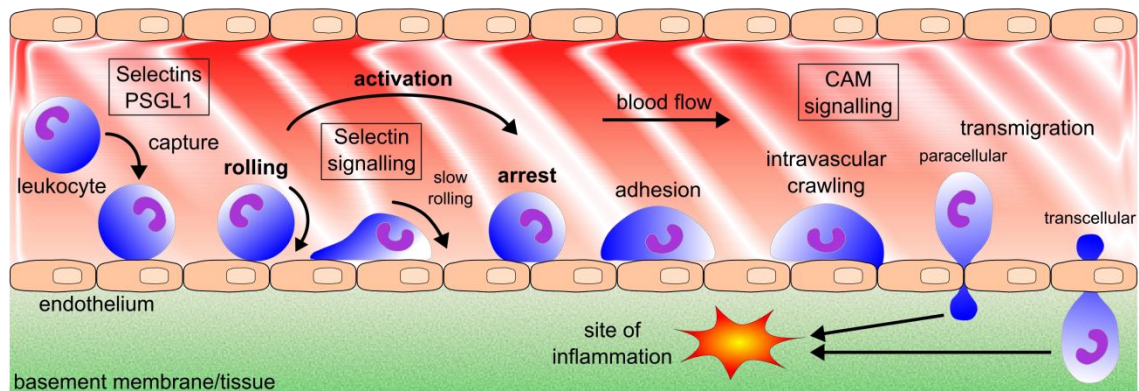


**Figure 7:** Schematic representation of the leukocyte recruitment from the blood stream including the leukocyte rolling via CAM, adhesion to the endothelium, and transmigration to the site of inflammation. Figure adapted from literature.<sup>[63]</sup>

The leukocytes circulating within the blood stream are recruited and captured on the vascular endothelium. Upon weak selectin-carbohydrate interactions with high on- and off-rates, the leukocyte starts to roll on the endothelial surface. During the rolling on the surface, the expression and activation of immunoglobulin receptors, e.g., ICAM1 and VCAM1 is triggered by chemokines and induces integrin-mediated leukocyte arrest, whereas the leukocyte binds firmly to the vascular endothelium.<sup>[64]</sup> Subsequently, the adherent leukocytes start intravascular crawling and subsequent transmigration.<sup>[63]</sup>

Based on scientific findings that revealed key steps of the inflammation cascade, it is now possible to design strategies to modulate leukocyte extravasation. Most of the studies conducted over the past three decades focused on the interaction between leukocytes and the vascular endothelium.<sup>[65]</sup> In order to prevent the initiation of the cascade, it is necessary to disturb the leukocyte recruitment from the blood stream. The most direct approach is to prevent the interaction of CAMs with the receptors presented on the leukocytes and therefore to inhibit the rolling on the vascular endothelium. This blocking imposes a structural knowledge about the selectins and their ligands involved in the recruitment process.<sup>[66]</sup> As discussed, selectins are subdivided into the classes L-, P-, and E-selectin in which the E-selectin is exclusively expressed at the endothelium upon a pro-inflammatory stimulation.<sup>[67]</sup> According to in vivo studies, the extravasation of leukocytes is proportional

to the presence and expression of selectins on the leukocytes or the vascular endothelium.<sup>[68]</sup> The down-regulation of the selectin receptors reduced the number of recruited leukocytes and consequently the immune response.

Various authors reported specific ligands for the binding of L-selectin (MAdCAM-1),<sup>[69]</sup> E-selectin (ESL-1),<sup>[70]</sup> and P-selectin (P-selectin glycoprotein ligand-1, PSGL-1).<sup>[67, 71]</sup> Independent from the selectin species, the receptors consist of five domains: the anchoring domain is located at the cytoplasm which is connected through a transmembrane region to the complement regulatory domains (CR). The number of the repeat units within this domain varies for each individual selectin species and consists of an epidermal growth factor (EGF)-like domain and a terminal carbohydrate recognition domain (CRD).<sup>[67]</sup> It was reported, that especially the binding properties of the lectin domain are crucial for the specific binding of selectin ligands.<sup>[72]</sup> Fundamental studies on the interactions of E- and P-selectins, identified distinct crystal structures of the receptors.<sup>[73]</sup> Extensive studies on PSGL-1 revealed a sulfated tyrosine residue in close proximity to a carbohydrate binding site to be important for the selectin binding.<sup>[74]</sup> Resulting from the crystal structure of PSGL-1 the scientific community accepts a general scheme for selectin ligands: all carbohydrate binding sites possess a distinct terminal oligosaccharide structure. This motif is based on a tetrasaccharide sialyl Lewis x (SiaLe<sup>x</sup>) and its structural isomer sialyl Lewis a (SiaLe<sup>a</sup>).<sup>[75]</sup> Despite the sialylated structure, the motif also bears the respective sulfated or non-sialylated structure: sulfo-Le<sup>x</sup>, sulfo-Le<sup>a</sup>, Le<sup>x</sup>, and Le<sup>a</sup>.

With the basic knowledge on how to disrupt the leukocyte recruitment during inflammatory processes, the main research focus was directed towards alternative structures for pan selectin ligand SiaLe<sup>x</sup>.<sup>[76]</sup> The strategy was based on blocking the selectin ligands with synthetic mimics to prevent leukocyte rolling on the vascular endothelium. Although a lot of synthetic ligands were evaluated, the main drawback of the low binding affinity of selectins to SiaLe<sup>x</sup> ( $k_d$  values in the low millimolar range) limited their potential use.<sup>[77]</sup> Recently, a study presented an E-selectin antagonist with a prolonged half-life in the nanomolar range.<sup>[78]</sup> Inspired by nature, the solution for low binding affinities for single receptor-ligand pairs was to mimic the leukocyte surface and the glycan clusters in physiological ligands.<sup>[79]</sup> Based on bi- and trivalent arrangement with distinct ligand separation, it was possible to address both, the aspects of low binding affinity and the size of the lectin domain (distance between tetrasaccharide moieties) of about 40 Å.<sup>[80]</sup> However, the increase in binding affinity upon oligovalent arrangement of

the ligands was small compared to the monomeric moiety. A multivalent presentation based on a liposome functionalized with SiaLe<sup>x</sup> was necessary to increase the binding affinity by approx. five orders of magnitude. A systematic study on SiaLe<sup>x</sup> and sulfo-Le<sup>x</sup> residues, which were embedded in liposomes with a distinct surface functionalization of sulfate esters, carboxylate, or hydroxyl functionality revealed that the binding affinity of the multivalently presented ligands is sensitive to the respective functional anionic groups.<sup>[81]</sup> The binding affinity ranged from the nanomolar for sulfates, over carboxylates, and neutral hydroxyl groups to the millimolar region for ammonium groups. This study indicated that anionic groups, especially sulfates, additionally to or instead of glycan motifs presented on the surface, provide a great potential for L- and P-selectin interactions.

The versatility of the general strategy of a multivalent arrangement of possible ligands was discovered with a liposomal approach: the affinity of SiaLe<sup>x</sup> to all three selectin ligands was utilized in a cytotoxic liposome equipped with additional merphalan which showed good antitumor activity in an in vivo mouse model.<sup>[82]</sup>

The following part illustrates the general concept of a common method to quantify the inhibition potential of especially polyanionic inhibitors. The main focus is directed towards multivalent inhibitors based on dPG and the systematic investigation of the structure-activity relationship.

### **1.2.3 Structure-Activity Relationship of Polyanionic Inhibitors**

#### **1.2.3.1 Characterization of the Anti-Inflammatory Properties**

The performance of selectin inhibitors and anti-inflammatory agents is generally expressed by binding affinities, or more explicitly, in IC<sub>50</sub> (inhibitory concentration) values. An IC<sub>50</sub> value describes the concentration at which 50% of the binding compared to a control sample is achieved. The measurement provides relative values and is strongly dependent on the experimental setup. Therefore, the comparison of binding affinities from literature is not always representing the biological situation, e.g., static assays do not consider the physiological shear stress present in the human circulatory system.<sup>[83]</sup> Nowadays, IC<sub>50</sub> values are usually performed under flow conditions with standardized equipment, such as surface plasmon resonance (SPR) devices.<sup>[84]</sup> Here, the shear rates present in the capillaries can be adjusted by varying flow rates in the SPR device. Hence, this in vitro-assay represents the physiological conditions with good approximation (see Figure 8).

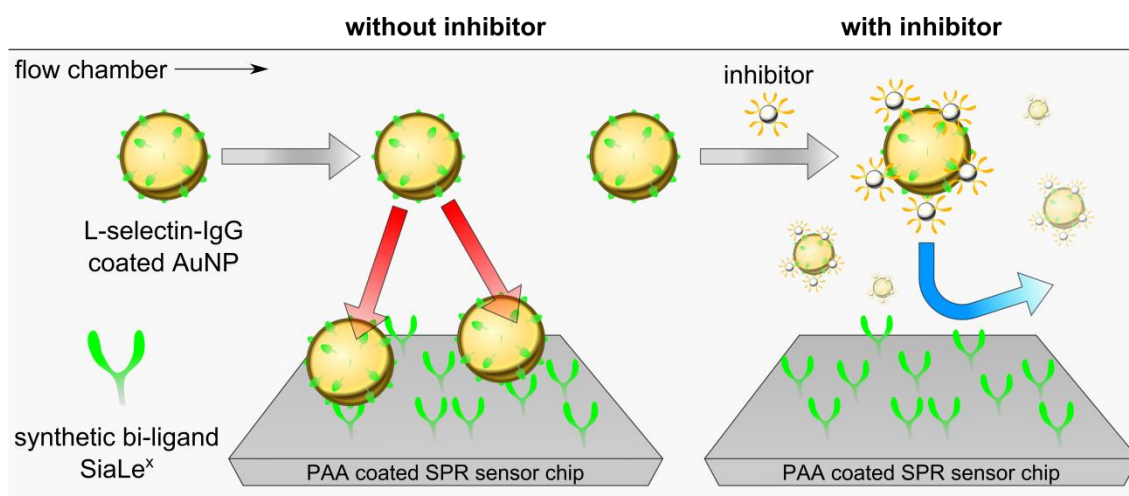


**Figure 8:** Schematic representation of a standardized competitive SPR-based selectin inhibition experiment. The  $IC_{50}$  values are determined relative to the control.

In a competitive SPR selectin inhibition assay, the surface of the sensor chip is covered with a synthetic selectin specific bi-ligand polymer which consists of the SiaLe<sup>x</sup> and sulfo-tyrosine binding motifs. Selectin-coated gold nanoparticles (AuNP), which represent the leukocyte in the blood stream, are passed over the sensor chip surface at a constant flow rate. Upon selectin-ligand interaction, the L-selectin coated AuNPs are captured and bind to the surface. Recorded resonance units are set to 100% binding (positive control). The performance of a potential inhibitor is quantified by a dose dependent preincubation with the selectin-coated AuNP. In case of no selectin binding of the residual compound, the resonance units remain unaffected and equal the positive control value. Otherwise inhibition reduces the binding signal.

### 1.2.3.2 Dendritic Polyglycerol Sulfates as Anti-Inflammatory Agent

The anti-inflammatory activity of anionically derivatized polysaccharides has been investigated since the late 1980s. Most of the studies focused on linear, sulfated glycans, e.g., heparin, dextran, and pullulan sulfate (see Figure 9).<sup>[85]</sup> Whereas heparin is a highly sulfated glycosaminoglycan, with the highest negative charge density among any naturally occurring macromolecules, sulfated dextran and pullulan have to be prepared from the respective neutral sugars.<sup>[86]</sup> The anionically derivatized glycans were successfully applied to the treatment of AIDS, sepsis, and human prostatic carcinoma *in vitro*.<sup>[87]</sup> However, there are well-known limitations for the application of heparin in polymer therapeutics.<sup>[88]</sup> As a naturally occurring product heparin is isolated from mammalian organs, which

renders a potential contamination with pathogens possible.<sup>[89]</sup> The high anti-coagulant and anti-thrombotic activity of heparin or analogues, and its application for the treatment of thromboembolic disorders since nearly one century, cannot camouflage the severe side effects which can occur. In order to achieve an anti-inflammatory effect and in vitro IC<sub>50</sub> values in a potential therapeutic window, the inhibitors have to be applied in high dosage over a long time period which can cause severe bleeding due to the anti-thrombotic and anti-coagulant activity.<sup>[8]</sup>

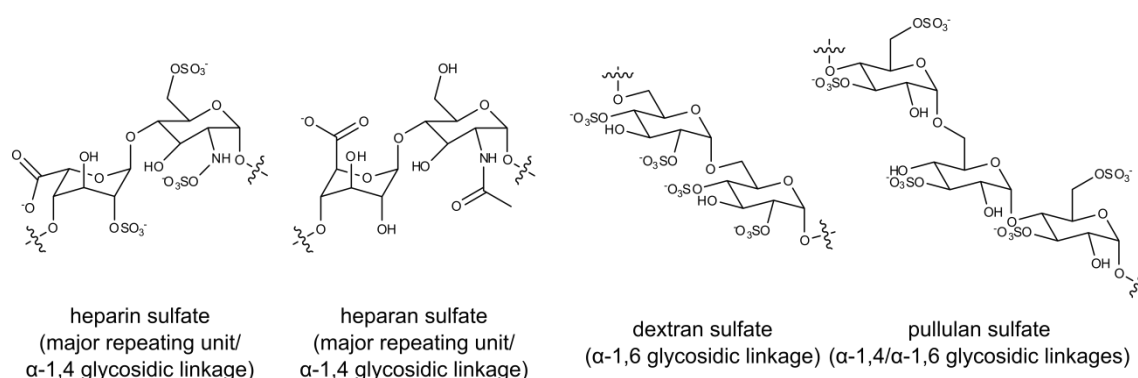


**Figure 9:** Structures of linear, anionic polysaccharides with anti-coagulant, anti-thrombotic activity and affinity towards L- and P-selectin.

However, the fundamental knowledge of the biological activity of anionic polysaccharides upon binding to proteins (e.g. antithrombin III) helped in the further development of anti-inflammatory agents.<sup>[90]</sup> The binding between the hydrophilic anionic polymers and proteins is usually based on electrostatic interactions of the ionic groups and hydrogen bonding.<sup>[91]</sup> Upon conformational arrangement, the polymeric inhibitors present their ionic groups usually on the surface and can bind to the respective protein with different multiple binding sites.

The described side effects of using naturally occurring polysaccharides for inflammation triggered the need for the development of fully synthetic, or semi-synthetic, highly sulfated polymer inhibitors with unique physicochemical properties. Therefore, various non-animal saccharide-based inhibitors were investigated for their selectin binding behavior, e.g., chitosan sulfate and dextran sulfate.<sup>[92]</sup> Upon chemical modification of polysaccharides to obtain heparin analogues, the glycans had distinct thrombin-mediating activity. An extensive study on sulfation of the carboxylated glycans determined that the anti-coagulating activity is reduced upon increasing the number of sulfate groups or degree of sulfation (DS), but at the same time the selectin binding to L- and P-selectins was preserved.<sup>[93]</sup> A combinatorial study on the effects of molecular weight (MW), and DS of

animal-derived, isolated sugars, i.e., unfractionated (UFH), medium molecular weight (MMWH), or low molecular weight heparin (LMWH), and semi-synthetic sulfated linear polysaccharide derivatives from phycarin, curdlan, and pullulan, revealed a distinct MW vs. DS relationship.<sup>[94]</sup> For a comparable surface charge density, there is no change in inhibitory activity above a certain MW threshold. The modulatory effect of the MW on the selectin inhibition was proven by the fact that larger molecular weight glycans required a lower DS for a similar performance in the biological assay.

The first study that described dendritic polyglycerol sulfate (dPGS) as heparin analogue mainly focused on three different core sizes of dPG with constant DS.<sup>[95]</sup> The sulfation was achieved by an efficient procedure utilizing a highly reactive sulfur trioxide-pyridine complex ( $\text{SO}_3\cdot\text{Pyr}$ ). The inhibition of the complement system and the anti-coagulating activity of the sulfated architectures was compared to neutral dPG, UFH, and a partially carboxylated dPG. The neutral and the carboxylated species were inactive in all conducted assays. The highly negatively charged dPGS significantly inhibited the classical complement activity (CCA) up to 23.9 times and prolonged the partial thromboplastin time (PTT), which describes both the intrinsic and the common coagulation pathways, up to 8.1% for the respective architectures. However, there was no clear tendency in the MW-activity relationship of the investigated structures.

Although not only saccharide based polyanions are known to show anti-coagulant and anti-inflammatory activity, most of the investigated architectures were based on linear polysaccharides. In 1998, Whitesides and coworkers presented their studies on polyvalent interactions for the design of multivalent ligands and inhibitors.<sup>[96]</sup> The bio-inspired observation that multiple ligand-receptor interactions, with individual low binding affinity contribute to strong overall binding of complementary surfaces broadened the perspective. Almost 15 years later, Haag et al. reviewed numerous results obtained from a collaborative research center, which is devoted to understand, evaluate, and model multivalent interactions.<sup>[59]</sup>

Papp and coworkers studied multivalent glycan-conjugates and covalently functionalized a dPG core with different saccharide moieties (see Figure 10). The azide-functionalized glycans were coupled to propargylated dPG by click-chemistry (1,3-dipolar cycloaddition). To emphasize the advantage of the multivalent PG scaffold, a galactose-tetramer was included into the assay. The structures were successfully tested as L- and P-selectin inhibitors.

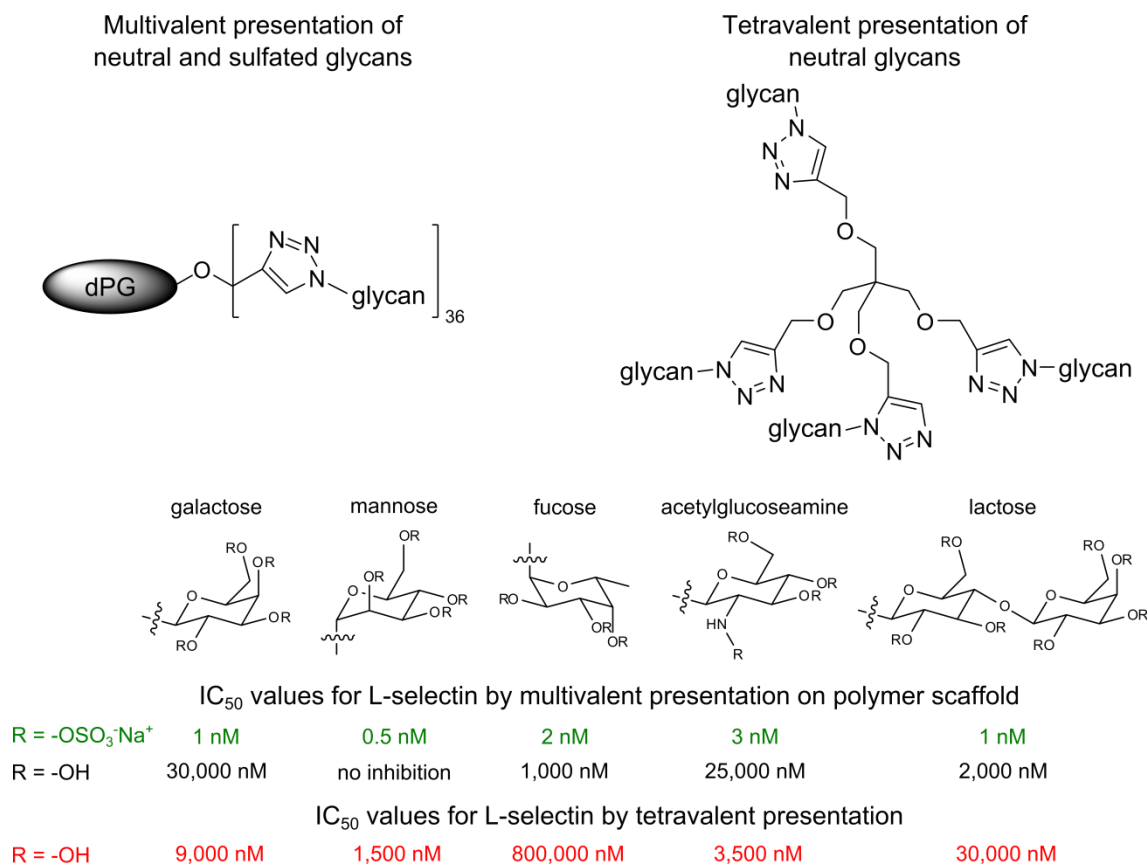


**Figure 10:** IC<sub>50</sub> values for multi- and tetravalently presented glycan displays on a polyglycerol and a pentaerythritol scaffold.

The specific selectin affinity of the multivalently presented, neutral glycans was enhanced up to 10<sup>3</sup>-fold (see Figure 10, black-colored IC<sub>50</sub> values) compared to the tetramer functionalized with the same glycans (see Figure 10, red-colored IC<sub>50</sub> values). For the presentation of the sulfated glycans the selectin inhibition was increased up to 10<sup>5</sup>-fold (see Figure 10, green-colored IC<sub>50</sub> values) compared to neutral tetramer species. The influence of the glycan moiety on the selectin inhibitory efficacy was further investigated in a consecutive study, where different non-sulfated and sulfated glycans were covalently attached to a dPG core.<sup>[97]</sup> The glycans  $\beta$ -D-galactose,  $\alpha$ -D-mannose,  $\alpha$ -L-fucose,  $\beta$ -D-N-acetylglucosamine,  $\beta$ -D-lactose, and the respective sulfate derivatives were multivalently presented by utilizing “click chemistry.” Similar to the first study, all PG-based polysaccharides were compared to the respective tetrameric glycan. The IC<sub>50</sub> values determined in the competitive SPR measurements showed an L- and P-selectin inhibitory enhancement of up to 10<sup>4</sup>-fold upon sulfation. The variation of the glycan display only



marginally affected the inhibition efficacy, as the  $IC_{50}$  values ranged from 0.5 nM for dPG-mannose-*O*-sulfate to 3 nM for dPG-acetylglucosamine-*O*-sulfate.

The studies on the sulfated PG-glycans emphasized the importance of the polyanionic nature for efficient L-selectin inhibition and the anti-inflammatory activity. Weinhart et al. extensively investigated different PG-based polyanions and correlated their binding affinity towards L-selectin to the nature of the anionic display (see Figure 11).<sup>[98]</sup> PG-based polyanionic architectures from cores with number average molecular weights ( $M_n$ ) of 3 000 g mol<sup>-1</sup> and 6 000 g mol<sup>-1</sup> were examined.

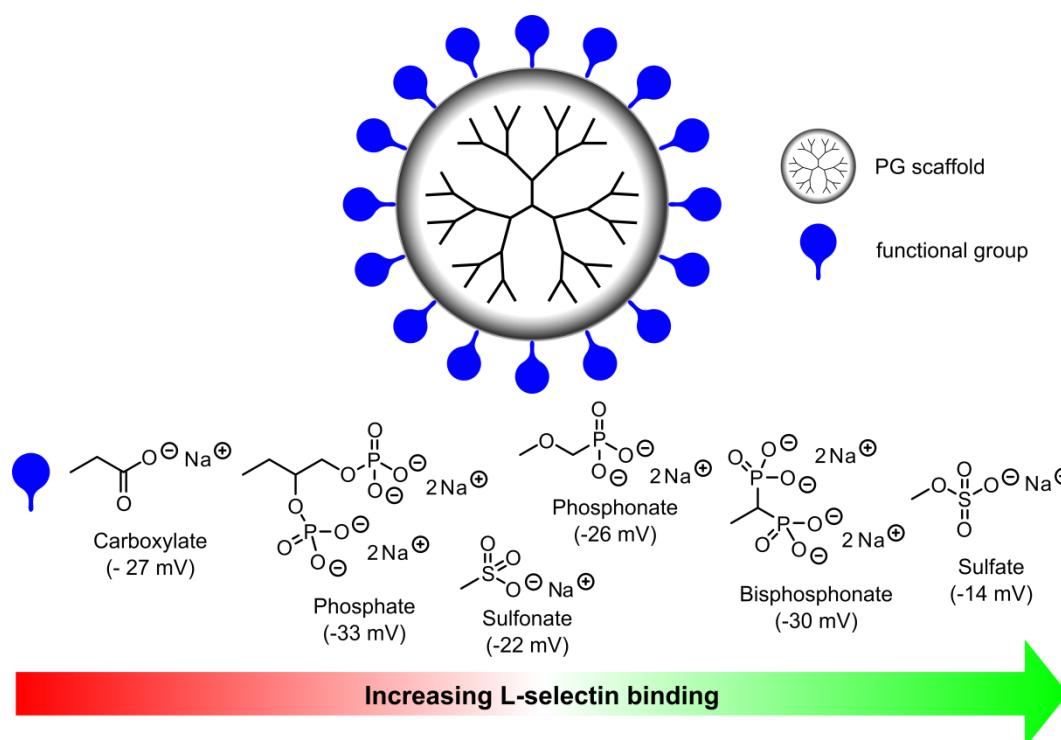


**Figure 11:** dPG-based anions and their affinity towards L-selectin. The  $IC_{50}$  values were investigated on different dPG core sizes of 3 000 and 6 000 g mol<sup>-1</sup> with a DF  $\geq$  81%. The L-selectin binding could not be directly correlated to the surface charge determined by  $\zeta$ -potential measurements (results given in brackets).

The anionic nature was varied by 1,3-dipolar cycloaddition of the sodium derivatives of prop-2-yne-1-sulfonate, prop-2-ynoxy methylphosphonate, but-3-yne-1,1-diylbisphosphonate, and 4-pentynoic acid, multivalently attached to dPG azide. The dPGS was synthesized according to the methodology described above and the dPG phosphate sodium salt (dPGP) was produced by direct interconversion of the hydroxyl groups. All architectures were obtained with comparable DF, particle size around 6 nm, and with  $M_n$  between approx. 7 000 g mol<sup>-1</sup> and 30 000 g mol<sup>-1</sup> for the respective functionalized

polyanions. The anionic character was determined by zeta potential ( $\zeta$ -potential) measurements in buffered solution at physiological pH 7.4. Interestingly, both dPGS species showed the most effective selectin inhibition with  $IC_{50}$  values of 16 nM and 8 nM, but the most positive  $\zeta$ -potentials of -5 mV and -14 mV, respectively. All other polyanions possessed an inhibitory efficacy from the medium nanomolar to the high micromolar range, although surface charge densities of -20 to -35 mV were determined. The results indicated that a direct correlation of the surface charge to the L-selectin inhibition seemed to be highly complex. The authors suggested a relationship between the protonation of the functional group which is dependent on the pH, the related binding strength of the sodium counter ion, and the formation of an ionic double layer on the polyelectrolyte surface to significantly influence the surface charge of the dPG-based polyanions. Therefore, the sodium ion binding in dPG carboxylate and the respective double layer is much smaller compared to dPGS, and in turn affects the surface charge under the investigated conditions. From the investigated functionalized dPG scaffolds, dPGS showed the highest L-selectin affinity with respect to molecular weight and particle size. However, as the differences in the particle sizes were negligible, the role of the polymer scaffold size and surface charge density on the L-selectin affinity was investigated more closely (see Figure 12).<sup>[99]</sup> According to the synthetic strategies described in Chapter 1.3.4, various dPG scaffolds with molecular weights from 2 000 g mol<sup>-1</sup> to 800 000 g mol<sup>-1</sup> were synthesized and sulfated. For the lower molecular weight dPGs ( $M_n < 100\,000$  g mol<sup>-1</sup>), three different DS, and for the high molecular weight dPGs only one high DS were investigated.

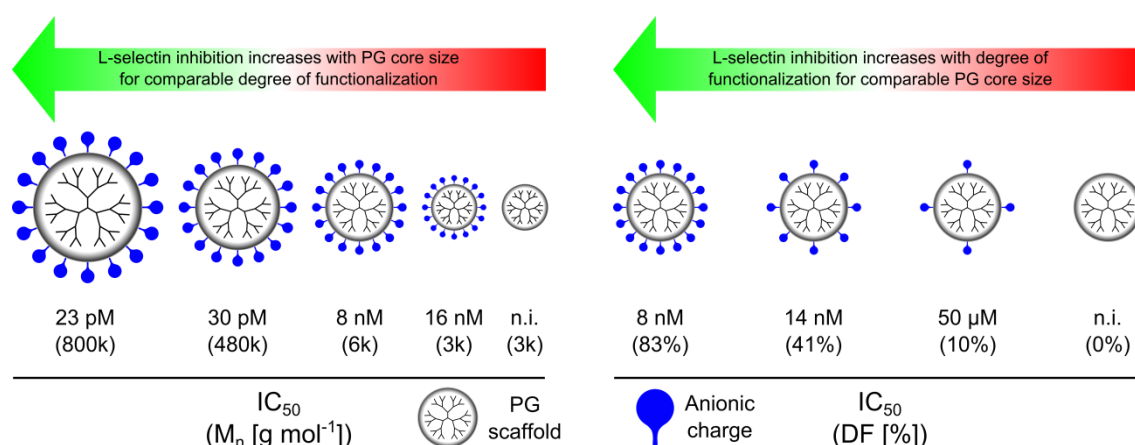


**Figure 12:** L-selectin inhibition of schematically illustrated, sulfated polyglycerol architectures. An enhanced inhibition potential was found for increased core size with similar degrees of functionalization (left), which is crucial for sufficient L-selectin affinity (right).

Depending on the particle size determined by dynamic light scattering (DLS), the smaller dPGSs with hydrodynamic diameters from 2 to 10 nm ( $M_n \leq 13\,000\text{ g mol}^{-1}$ ) showed  $IC_{50}$  values from 100 to 8 nM. The  $\zeta$ -potential ranged from -1.5 to -13.6 mV. The surface charge of the larger dPGS with diameters above 10 nm ( $250\,000 \leq M_n \leq 1\,800\,000\text{ g mol}^{-1}$ ) was about three times smaller than what was expected for the increased number of sulfates. With the larger dPGS, the L-selectin affinity was enhanced to an  $IC_{50}$  value of 23 pM for a particle size of 17 nm. Interestingly, the change of the inhibitory effect from 250 000 to 1 800 000  $\text{g mol}^{-1}$  was increased only 8-fold compared to a 13-fold enhancement from 4 300 to 13 000  $\text{g mol}^{-1}$ . This improvement can be attributed to a surface charge threshold which seems to be reached for the large particles. A second threshold for the DF was further determined to be around 70 to 80% sulfation. All studies on anionically derivatized dPGs, either via attachment of sulfated saccharides and anionic moieties or direct conversion of the hydroxyl groups, clearly determined that the surface charge density and the nature of the anionic display are crucial for the anti-inflammatory activity. However, to further characterize the structure-activity relationship of dPGS regarding its L-selectin affinity, it is necessary to systematically investigate the structural influence of the polymer backbone itself, e.g., by variation of the flexibility and the branching, respectively.

The results presented in Chapter 1.1 and 1.2 illustrate the great potential of applying hyperbranched polymers and especially dPG in polymer therapeutics. The following Chapter 1.3 will present the historical development of hyperbranched polymer synthesis and especially focuses on dPG including the state-of-the-art in dPG polymerization with different methodologies.

### 1.3 Synthesis of Dendritic Polymers

#### 1.3.1 Polymer Architectures

Hyperbranched polymers are classified as tree-like macromolecules and belong to the class of dendritic polymers.<sup>[100]</sup> In general, dendritic polymers can be divided into six subclasses: (a) dendrimers, (b) dendritic–linear hybrids, (c) dendrigrafts/dendrigrafted polymers, (d) hyperbranched polymers, (e) star-shaped–linear hybrids, and (f) hypergrafts/hypergrafted, as presented in Figure 13.

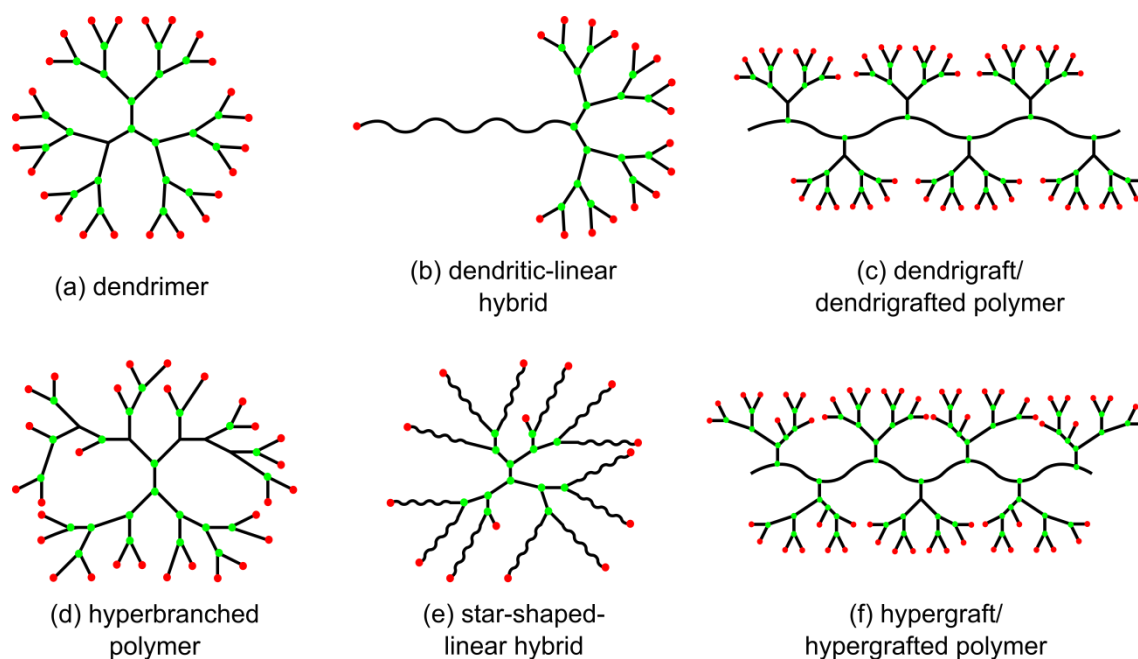


**Figure 13:** Schematic overview of the subclasses of dendritic polymer architectures: (a) dendrimer, (b) dendritic–linear hybrid, (c) dendrigraft/dendrigrafted polymer, (d) hyperbranched polymer, (e) star-shaped–linear hybrid, (f) hypergraft/hypergrafted polymer. Branching (green) and terminal groups (red) are indicated.

For better comparison of the structural differences, the branching points are depicted in green and the terminal/functional groups in red. The first three subclasses (Figure 13, (a)–(c)) are perfectly branched structures with  $DB = 100\%$  which are generally synthesized via tedious, multistep procedures. The monodisperse structures are synthesized in a convergent or divergent approach and consist of different layers or generations, respectively. Tedious workup of each generation is required. The subclasses containing hyperbranched elements (Figure 13, (d)–(f)) are usually manufactured in a more facile, one-pot synthetic approach, resulting in  $DB$ s between 0 and 60%.

The structures presented in Figure 13 are different from the well-known classes of (a) cross-linked polymer network, (b) branched, and (c) linear polymer architectures, which are schematically represented in Figure 14.<sup>[101]</sup>

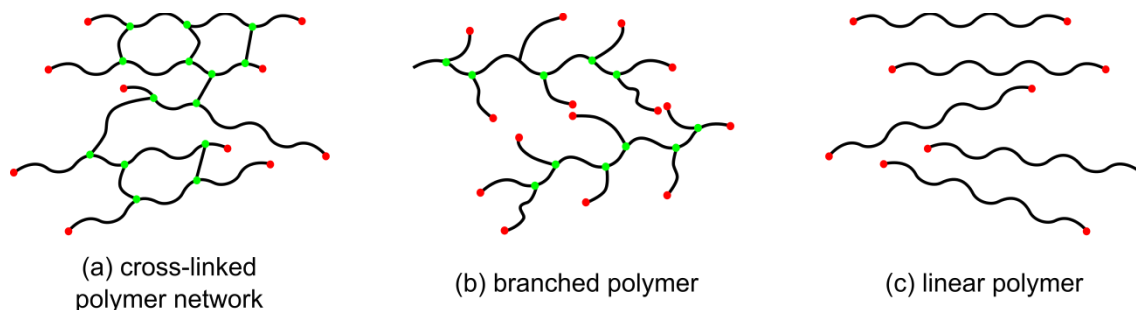


**Figure 14:** Schematic representation of classical polymer structures with (a) cross-linked polymer network, (b) branched polymer, and (c) linear polymer structures. Net points (green) and terminal groups (red) are indicated.

Dendritic polymers exhibit defined hydrodynamic diameters and surface functionalities with respect to their DB. The perfectly branched structures (a), (b), and (c) in Figure 13 possess no internal functional groups but are fully surface functionalized with regard to the dendritic part (linear compartments are not considered). With their predominantly spherical structure, a high surface functionality, a distinct hydrodynamic diameter, dendritic and hyperbranched polymers represent a class of molecules with unique chemical and physical properties, e.g., solution viscosity and aggregation behavior, which are considerably different from the classic polymer architectures shown in Figure 14.<sup>[102]</sup>

The following Chapter will focus on hyperbranched polymers manufactured by different synthetic methodologies. Additional information on the monomers for different synthetic methodologies and general applications for hyperbranched polymers will be discussed.

### 1.3.2 Hyperbranched Polymers

The seminal report on hyperbranched polymers was published at the beginning of the 20<sup>th</sup> century when the resin formation from an  $A_2B_2$  (tartaric acid), and a  $B_3$  monomer (glycerol) was reported.<sup>[103]</sup> The monomers were classified by the nature of the functional group  $A_x$  with the index  $x$  representing the number of functional groups per monomer. Tartaric acid contains two carboxylic acid  $A_2$  and hydroxyl groups  $B_2$ , and glycerol provides three hydroxyl groups  $B_3$ . The study described the reaction between phthalic anhydride (latent  $A_2$  monomer) or phthalic acid ( $A_2$  monomer), respectively, with glycerol

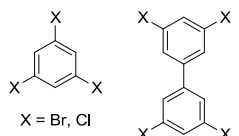
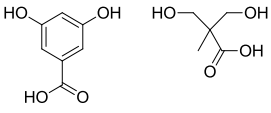
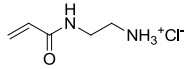
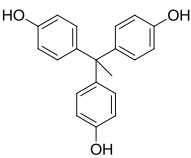
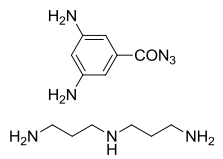
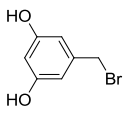
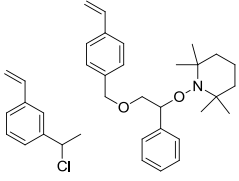
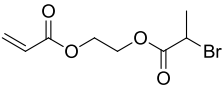
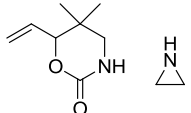
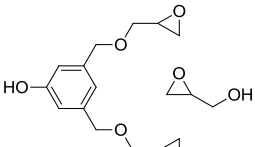
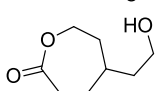
(B<sub>3</sub> monomer), and it was determined that the specific viscosity of the branched A<sub>2</sub>B<sub>3</sub> products was different compared to the values for linear polystyrene and indicated special structural properties.<sup>[104]</sup> This method was later referred to as the double-monomer methodology (DMM), in which the hyperbranched structure is built by the polymerization of orthogonally functionalized monomers.<sup>[105]</sup> The first industrial synthetic plastic and commercially available polymer with a so-called randomly hyperbranched structure, was introduced by Baekeland.<sup>[106]</sup> The cross-linked phenolic polymer resins were polymerized from resole precursors which were made from formaldehyde (latent A<sub>2</sub> monomer) and phenol (latent B<sub>3</sub> monomer).

In the beginning of the 1940s, Flory published his first theoretical calculations on three-dimensional polymers with respect to the incorporation of tri- and tetra-functional branching units and their effect on the molecular weight distribution.<sup>[107]</sup> In 1952, Flory reported his concepts on ‘degree of branching’ and ‘highly branched species’.<sup>[108]</sup> In addition, he suggested a polycondensation mechanism for highly branched structures using an AB<sub>n</sub> monomer ( $n \geq 2$ ).

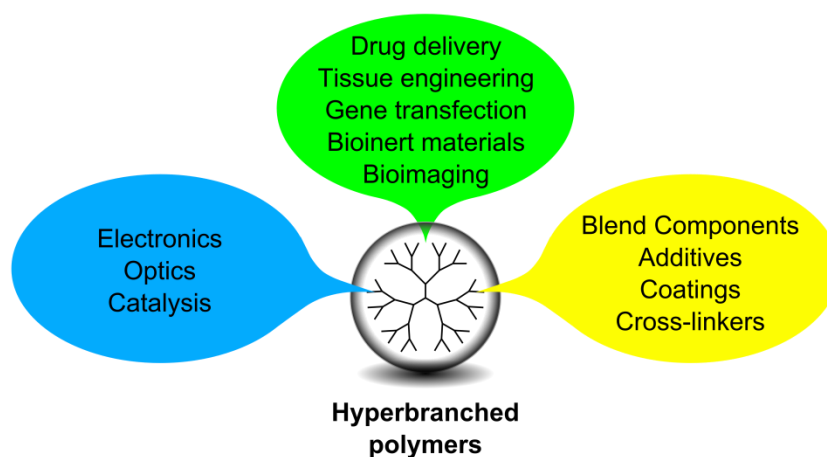
Based on Flory’s suggestions, the copolymerization of 3-acetoxy benzoic acid (AB monomer) and 3,5-(bisacetoxy)benzoic acid (AB<sub>2</sub> monomer) yielded the first highly branched polyesters in 1982.<sup>[109]</sup> The term ‘hyperbranched polymer’ was finally introduced in 1988 with the synthesis of carboxylate functionalized polyphenylene as a soluble, hyperbranched polymer made from an AB<sub>2</sub> monomer.<sup>[110]</sup> This approach was described as the single-monomer methodology (SMM), with the subclass (a) ‘polycondensation of AB<sub>2</sub> monomer’. The other subclasses developed in the following decade are referred to as (b) ‘self-condensing vinyl polymerization’ (SCVP),<sup>[111]</sup> (c) ‘self-condensing ring-opening polymerization’ (SCROP),<sup>[112]</sup> and (d) ‘proton-transfer polymerization’ (PTP).<sup>[113]</sup>

Table 1 presents a summary of classical hyperbranched and commonly applied architectures, including their preparation method, applicable monomers, and the pioneering authors who developed the systems and conducted the fundamental research that science and industry are benefiting from today.

**Table 1:** Selected hyperbranched polymers with the specific synthetic methodology for their preparation, applicable monomers, and possible applications.

Polymer class	Applicable monomers	Authors
<i>SMM – Polycondensation of AB<sub>n</sub> monomers</i>		
Polyphenylenes		Kim & Webster <sup>[114]</sup> Morgenroth & Müllen <sup>[115]</sup>
Polyesters		Hawker & Fréchet <sup>[116]</sup> Malmstroem & Hult <sup>[117]</sup>
Polyamides		Hobson & Feast <sup>[118]</sup>
Polycarbonates		Bolton & Wooley <sup>[119]</sup>
Polyureas, Polyurethanes		Kumar & Meijer <sup>[120]</sup>
Polyethers		Uhrich & Fréchet <sup>[121]</sup>
<i>SMM – SCVP of AB* monomers</i>		
Polystyrenes		Fréchet, Grubbs, Hawker <sup>[111, 122]</sup>
Polymethacrylates, Polyacrylates		Coessens & Matyjaszewski <sup>[123]</sup>
<i>SMM – SCROP + PTP of AB<sub>x</sub> monomers</i>		
Polyamines		Saegusa & Suzuki <sup>[112a, 124]</sup>
Polyethers		Chang & Fréchet <sup>[113]</sup> Frey & Haag <sup>[26b, 125]</sup>
Polyesters		Fréchet & Liu <sup>[126]</sup>

The summary in Table 1 provides a first indication of the variety of the available hyperbranched polymers nowadays. Polyphenylene architectures are generally used as thermal stability modifiers, advanced coating systems, and in organic electronics.<sup>[114-115, 127]</sup> Polyureas and polyurethanes (precursor) are especially applied for automotive and housing applications as, e.g., foaming agent, adhesive, filler, and cross-linker.<sup>[120]</sup> The hyperbranched aliphatic polyesters from the AB<sub>2</sub> monomer 2,2-bis(hydroxymethyl propionic acid) (bis-MPA) developed by Hult and coworkers,<sup>[117]</sup> are commercially available under the tradename Boltorn<sup>TM</sup> and classified as a high performance polymer. Another economically important hyperbranched polymer is PEI which is used for various applications in industry and research, e.g., as engineering polymer, transfection agent, flocculating agent, or soluble support, due to its outstanding foaming, complexation, and solubility properties.<sup>[128]</sup> An overview of common industrial and research applications for hyperbranched polymers is presented in Figure 15.



**Figure 15:** General applications of hyperbranched polymers in industry and research.

Although a lot of research in biomedicine is focused on dendritic architectures, most of the polymers share a tremendous disadvantage which is their reduced biocompatibility and increased toxicity. Based on the unique properties of dPG, which was extensively discussed in Chapter 1.1 and 1.2, it represents a potential alternative to other hyperbranched architectures. The following chapter provides insight into the historical development of dPG and the pioneering work of various scientists which is the basis for the state-of-the-art in dPG synthesis presented here.



### 1.3.3 Historical Development of Hyperbranched Polyglycerols

Already at the early stage of development, glycidol was investigated as a potential monomer for the synthesis of branched species. With the latent AB<sub>2</sub> monomer exhibiting an epoxide and a hydroxyl group, Sandler and Berg first reported the polymerization of glycidol with various catalysts.<sup>[129]</sup> The catalyst [e.g., triethylamine (TEA), pyridine, potassium hydroxide (KOH), or sodium methoxide (NaOMe)] was suspended in the monomer and the mixture was stirred at room temperature for several days. For some initiators, e.g., NaOMe as well as pyridine at  $c = 1$  wt%, low-molecular weight oligoglycerols with  $M_n < 500 \text{ g mol}^{-1}$  were detected. For other initiators, e.g., TEA and KOH, changes in the inherent viscosity  $\eta_{\text{inh}}$  compared to the pure monomer were found. A base-catalyzed anionic polymerization mechanism was proposed for the growth of oligoglycerols without consideration of branching. In 1985, the anionic polymerization of glycidol was investigated in more detail, using KOH and potassium *tert*-butoxide (KO*t*Bu) as initiators.<sup>[130]</sup> The branched structures were characterized by <sup>13</sup>C-NMR spectroscopy and the branching was explained by a PTP mechanism. The reported polyglycerols were obtained with weight average molecular weights ( $M_w$ ) of approx.  $2\,000 \text{ g mol}^{-1}$ . In 1994, Tokar and coworkers utilized the initiators boron trifluoride diethyl etherate (BF<sub>3</sub>·OEt<sub>2</sub>), hexafluorophosphoric acid-ether complex (HPF<sub>6</sub>·OEt<sub>2</sub>), and tin(II) chloride (SnCl<sub>2</sub>) for the cationic polymerization of glycidol.<sup>[131]</sup> Although cationic reaction conditions at low temperature were applied, only oligoglycerols were obtained. A study on the reactivity of epoxy model compounds with amines at different temperatures and without solvent revealed that the reactivity at 20 °C is too low for most of the derivatives which were used.<sup>[132]</sup>

Due to an increasing interest in hyperbranched polymers in the scientific community, Frey and coworkers conducted topological investigations on AB<sub>2</sub>, AB<sub>3</sub>, and AB<sub>m</sub> ( $m \geq 2$ ) monomers,<sup>[133]</sup> which finally resulted in the development of the slow monomer addition technique (SMA) at the end of the 20<sup>th</sup> century.<sup>[134]</sup>

Starting from theoretical considerations on the relationship between monomer addition speed versus molecular weight and branching, Frey and Haag utilized the ring opening multibranching polymerization (ROMBP) of the latent glycidol monomer to synthesize dPG on large scale.<sup>[125, 135]</sup> The ROMBP represents a combination of the SCORP and the PTP mechanism; both of which belong to the SMM methodology (see Figure 16).<sup>[26a]</sup> A benefit of this approach is the utilization of a latent AB<sub>2</sub> monomer, i.e., one of the B-functionalities is inactive until one A and B of two different monomers react with each

other. In an ideal setup without moisture and self-initiation, the second B-functionality is liberated upon epoxide opening and can react further. From theoretical considerations, the system is classified as a living system. In reality, however, a large number of factors influence the ROMBP system based on the SMA technique and will be discussed within the context of the presented results. In Figure 16, the reaction steps of initiation and propagation are generally assigned to distinct reaction steps, and are different from the classical mechanisms which are known from radical or ionic polymerization. Here, the first attachment of a monomer to the initiator is considered as the initiation step. Subsequent attachment of monomer is described as propagation steps.

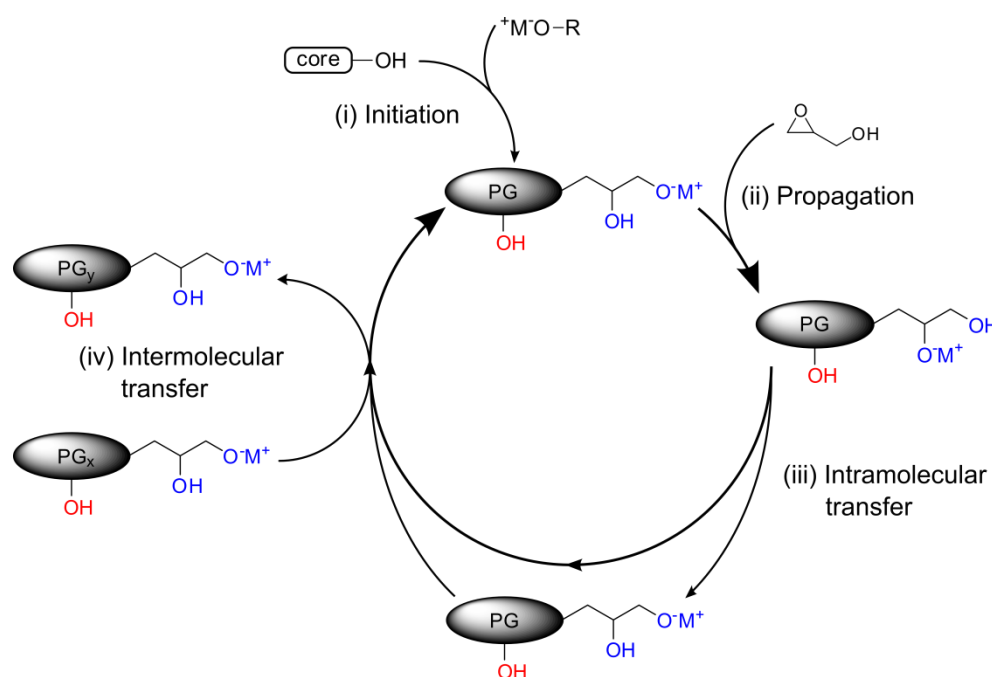


**Figure 16:** Schematic representation of the ROMBP mechanism, including (i) deprotonation/initiation, (ii) propagation upon SMA, (iii) intramolecular, and (iv) intermolecular proton transfer. Scheme adapted from literature.<sup>[26a]</sup>

With its highly functional, biocompatible polyether backbone, dPG is an alternative to perfectly branched dendrimers.<sup>[26b]</sup> Nowadays, dPG is used in numerous applications, e.g., as catalyst support,<sup>[136]</sup> as building block of biodegradable scaffolds,<sup>[137]</sup> and in polymer therapeutics.<sup>[138]</sup> The use of dPG as scaffold in a wide range of applications (described in Chapter 1.1 and 1.2) is based on the versatile toolbox system (see Figure 17). The dPG scaffold can exhibit unique properties by fine tuning of the functional monomers, bi-functional initiators, and the distinct surface functionalization.<sup>[26a]</sup> The toolbox system is extremely variable, i.e., the different building blocks are mostly independent from each other. This opens the possibility for dPG with two or three distinct functionalities, e.g., a

clickable core, with a hydrophobically derivatized backbone and a hydrophilic surface functionality.

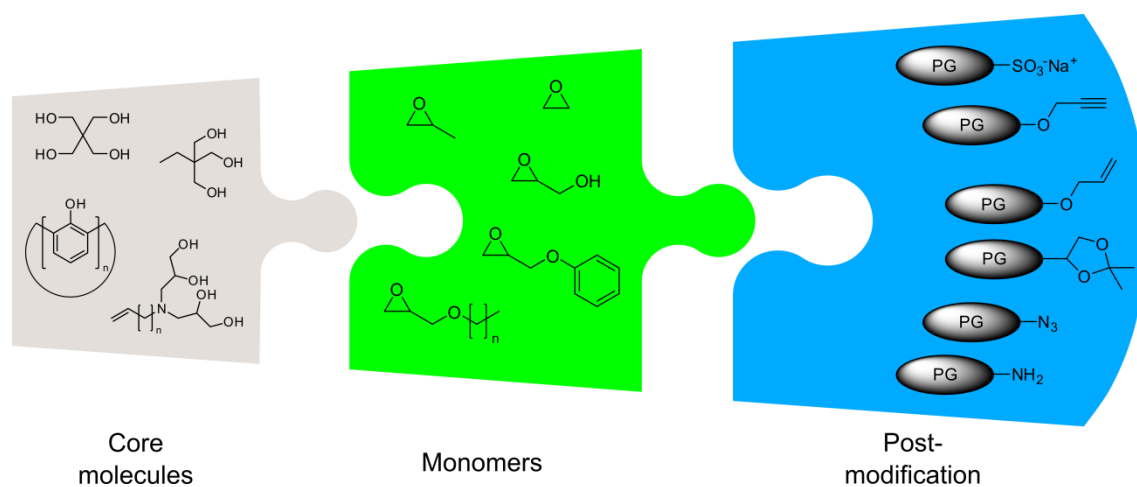


**Figure 17:** The dPG toolbox system – selective chemical differentiation by utilizing functional initiators, (co-)monomers, and surface functionalization to create polymers with unique properties. Scheme adapted from literature.<sup>[26a]</sup>

### 1.3.4 State-of-the-Art in Polyglycerol Synthesis

Since the discovery of dPG and its unique properties, many studies focus on its application. However, the dPG synthesized by the SMA method introduced by Frey and Haag was determined to have certain limitations with regard to the molecular weight distribution (MWD). The dispersity index (DI) was determined to significantly increase with increasing molecular weight above  $10\,000\text{ g mol}^{-1}$ .<sup>[139]</sup> In consequence, the accessible hydrodynamic particle size is restricted to approx. 6 nm. For instance, the limited core size cannot cover all fields addressed in nanomedicine, e.g., regarding the ADME behavior which is dependent on size, surface charge, chemical modifications, or surface morphology.<sup>[4a, 16b]</sup> The request for dPG with particle sizes from the nanometer to the low micrometer range amplified the need for new PG-based architectures and triggered the development of new synthetic strategies (see Figure 18).<sup>[140]</sup>

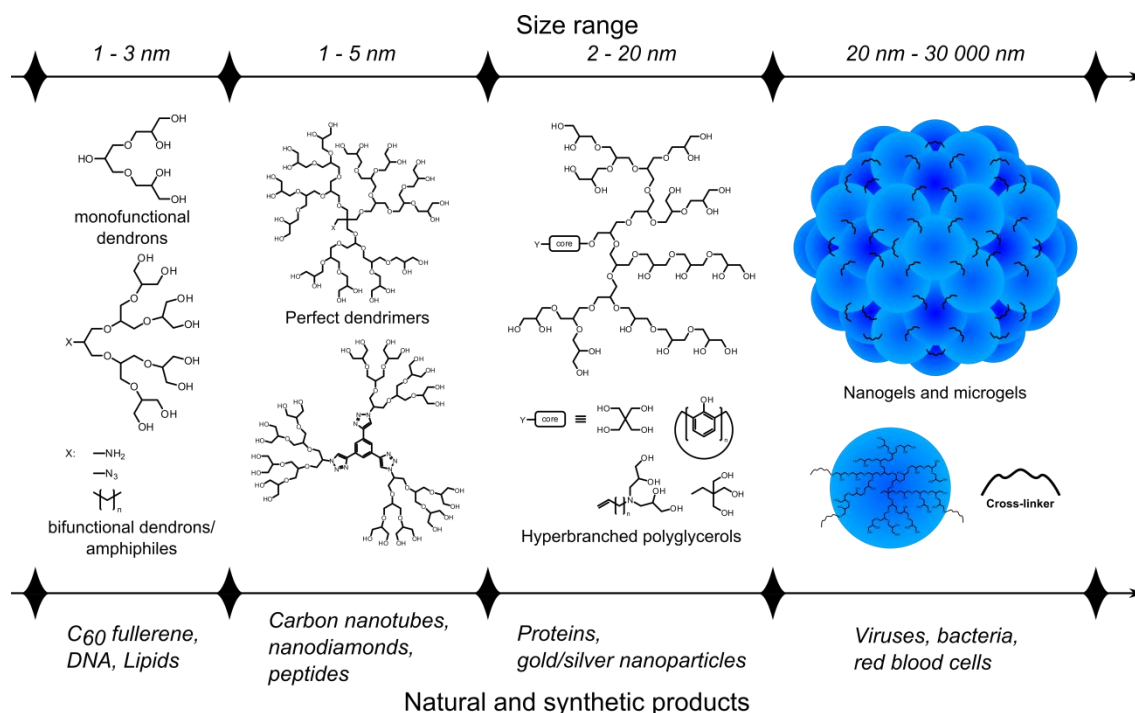


**Figure 18:** Different PG-based architectures with particle sizes from 1 nm to 30  $\mu\text{m}$  for applications in polymer therapeutics, and comparable other natural and synthetic products in the same size range. Figure adapted from literature.<sup>[140]</sup>

A direct approach towards higher molecular weights utilized dPG macroinitiators which provide a higher number of functional groups compared to a low molecular weight initiator and therefore an increased degree of deprotonation (DD), assuming no or less side reactions.<sup>[141]</sup> dPG with molecular weights of up to 24 000  $\text{g mol}^{-1}$  with dispersities between 1.3 and 1.8 were synthesized using 500 and 1000  $\text{g mol}^{-1}$  PG-based initiators. Brooks and coworkers prepared high molecular weight dPGs with up to 800 000  $\text{g mol}^{-1}$  by applying a solvent-assisted, pseudo-emulsion polymerization strategy, in which neither monomer nor polymer were soluble in the applied solvent.<sup>[142]</sup> By utilizing different solvents and solvent/monomer ratios, the achieved molecular weights were explained by variation of the reactivity upon counter ion complexation of the solvent.<sup>[143]</sup> However, the underlying mechanism is not fully elucidated and still under investigation.

The excretion/elimination mechanism of administered particles has become of great interest over the past years. On one hand it is important to benefit from high molecular masses and the EPR effect, but on the other hand the described ADME behavior is a limiting factor. In this context, the accumulation of high molecular weight PG (above the

renal excretion threshold) in the liver presents a challenging topic.<sup>[144]</sup> This issue can be addressed by the incorporation of cleavable units into the polymer scaffold.<sup>[145]</sup> Two synthetic strategies for biodegradable polymers were recently published. A dPG with biodegradable ester groups was synthesized by a hybrid polymerization of the hetero-bifunctional monomer glycidyl methacrylate (GMA) with glycidol.<sup>[137a]</sup> By applying the comonomer GMA, it was possible to propagate the reaction oxyanionically over both the double bond and epoxide functionalities. The final polymer degraded under distinct acidic conditions via an ester cleavage. Similar to the macroinitiator strategy, a biodegradable dPG with a star-shaped macroinitiator was designed by Kizhakkedathu and coworkers.<sup>[137b]</sup> The cleavable core was synthesized by a multistep approach and functionalized with dPG according to the ROMBP mechanism. Although the sizes of both the polymer and degradation products were below a pharmacologically relevant threshold, the general strategy offers great potential for bioconjugation applications.

The versatile nanogel methodology was developed to address the need for larger PG-based nanoparticles (see Figure 18, right section). Recently, Haag and coworkers published a strategy to synthesize gels in various dimensions based on functionalized dPG precursors.<sup>[146]</sup> The acrylated macromonomers were processed by mini-emulsion and microfluidic templating. A thermoresponsive PG-based nanogel was manufactured by crosslinking PNIPAm with small amounts of acrylated dPG.<sup>[147]</sup> The hydrodynamic size was reversibly switchable between 80 and 160 nm depending on the environmental temperature. Regarding the ADME behavior of synthetic nanoparticles especially in the micrometer range, biodegradability is essential. A nanoprecipitation-based biodegradable PG nanogel, which was synthesized by click coupling of functional dPG precursors, allowed for efficient encapsulation and release of various guest molecules.<sup>[137c]</sup> From the selected examples of dPG applications, the need of high-quality and biocompatible dPG is obvious.

In order to understand the ROMBP process in more detail and discover further fields for optimization, the following section provides a brief insight into the basic kinetics of the PG polymerization applying the SMA technique in comparison to the classical polymerization mechanisms.

### 1.3.5 Basic Principles for Polymerization Mechanisms and Kinetics

The knowledge of the polymerization mechanism is a crucial requirement to determine opportunities to influence this polymerization process in order to improve the quality, the yield, and the efficiency of a synthetic process. In general, any polymerization is based on either a step-growth or a chain-growth mechanism.<sup>[101]</sup> Based on the two principles, the kinetics of the processes differ fundamentally and different aspects are more or less important to synthesize high quality polymers in a reproducible fashion. For the step-growth mechanism, which implements an addition and condensation mechanism, it is important to achieve high conversions and to apply balanced monomer feed ratios of 1:1 for AABB systems, which is of less importance for AB systems. Especially for the polycondensation, it is important to remove the condensation by-product, e.g., by evaporation and/or neutralization to shift the chemical equilibrium. In general, the system is best described by the Carothers equation for the relationship between conversion and molecular weight.<sup>[101, 148]</sup> On the other hand, chain-growth polymerizations are fundamentally different. With an anionic, cationic, free-radical, controlled-radical, or coordinative growth mechanism, the reaction is influenced by many aspects. For a free-radical polymerization, it is important to quench the reaction at an early stage in order to avoid uncontrolled conditions.<sup>[149]</sup> In contrast, an ionic growth mechanism is considered a “living” polymerization with slowly and uniform propagating chains.<sup>[150]</sup> In this “living” type of polymerization, the ratio of monomer to initiator is directly proportional to the target molecular weight, and generally not susceptible to side reactions, when the monomers are purified beforehand and the reaction conditions are adjusted accordingly.<sup>[101]</sup> In controlled-radical polymerizations, only a small amount of monomer or growing chain is in an active state. The majority is in a “dormant” state. At periodic intervals, every monomer is activated upon a chemical equilibrium. However, side reactions can occur in controlled-radical polymerizations and therefore it is not considered a “living” type of polymerization.

The PG synthesis under SMA conditions, which was introduced by Frey and Haag and extensively discussed in Chapters 1.3.3 and 1.3.4, is based on such a “living” mechanism.<sup>[125, 151]</sup> However, the ROMBP mechanism (see Figure 16) is more susceptible for side reactions, which disturb the uniform growth and consequently reduce the quality of the final polymer. This lack of control results from the glycidol monomer, which can thermally add to other monomers in an uncontrolled fashion. Although a base-mediated propagation is expected, the high reaction temperatures of approx. 120 °C may be high

enough for thermal propagation by a ring-opening reaction of the three-membered, highly reactive epoxide ring. This side-reaction is comparable to the thermal propagation in a vinyl polymerization at high energy input, e.g., high reaction temperatures.<sup>[152]</sup> In comparison to the transfer-to-monomer side reaction, glycidol as a latent AB<sub>2</sub> monomer can be deprotonated (accept a counter-ion) and act as an initiator, which is also classified as uncontrolled side reaction. The discussed reactions render the “living” character of the ROMBP mechanism to “pseudo-living”. However, it is essential to further study the kinetics of the PG polymerization to gain a deeper understanding of the limitations of the process and to provide high quality polymers.

## 2 Scientific Goal

As described in the introduction, dendritic polyglycerol (dPG) exhibits unique physicochemical properties and is applied in numerous biomedical applications. Consequently, the demand for polyglycerols with constant high quality is increasing and therefore it is even more important to understand the kinetics and parameters which influence its synthesis, which is the main goal of this work. This knowledge will help to develop a highly reproducible process for the synthesis of high-quality dPGs. In the first part of this work, the large scale polymerization of dPG will be investigated in more detail and in particular with regard to the contribution of thermal and base-mediated propagation to the final molecular weight distribution (see Figure 19).

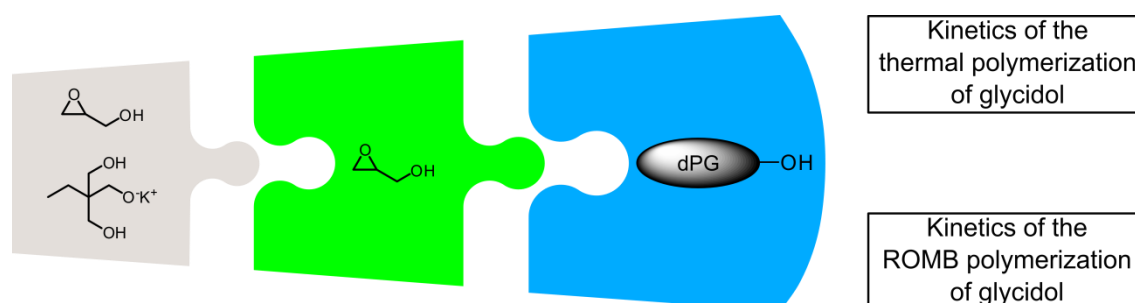


**Figure 19:** Investigation of the thermal polymerization of pure glycidol and the base-catalyzed ROMB polymerization of glycidol onto a TMP initiator.

The reaction mixture will be probed at regular intervals, and subjected to GPC and NMR analytics. In a second study, the complete process, including initiator and base-catalyst, will be investigated for three different molecular weights, according to the same protocol. An extensive parameter simulation will be conducted to establish a model with defined reaction coefficients to model all experimental data.

Previous studies on anti-inflammatory dendritic polyglycerol sulfates (dPGS) revealed a distinct structure-activity relationship with respect to the functionalization and the size of the polymer scaffold.<sup>[99]</sup> In order to extend the knowledge of this relationship, the second part of this work will focus on the derivatization and biomedical application of dPGS utilizing the flexible polyglycerol toolbox system. The synthesis will be manipulated by the addition of a protected comonomer to the monomer feed, which can introduce linear branching units only. This will reduce the degree of branching (DB) from approx. 60% to an intermediate value, depending on the monomer feed ratio. After deprotection and functionalization the evaluation will be performed by different biological assays, i.e.,



cellular uptake, competitive SPR measurements, and blood compatibility studies of sulfated and dye labeled polyglycerols with intermediate to 100% DB.

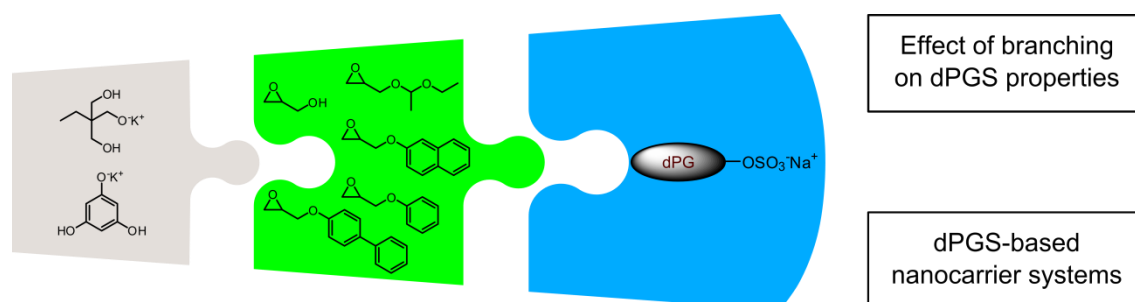


**Figure 20:** The polyglycerol toolbox system for the synthesis of derivatized polyglycerol sulfates with (i) different DB and (ii) hydrophobic moieties.

As described in the introduction, unimolecular core-shell (CS) and core-multishell (CMS) nanocarriers are highly potent drug delivery systems (DDS) which are able to transport guest molecules over biological barriers to specific targets. Numerous dendritic polymers have been investigated as scaffold for DDS. With its toolbox system, dPG can be easily modified to exhibit host properties. In the third part, different hydrophobically derivatized dPGSs will be investigated as nanocarriers with anti-coagulant and anti-inflammatory properties. The flexible toolbox system will be manipulated by including three aromatic-derivatized glycidol monomers. In one polymer library, the hydrophobic moieties will be exclusively positioned in the core by a core-first synthetic approach. For the second library, it will be randomly distributed over the whole hydrophilic PG matrix by polymerization with defined monomer feed ratios. The biological evaluation of the sulfated copolymers will be conducted with representative human cancer cell lines in both fluorescence activated cell scanning (FACS) assays and confocal laser scanning microscopy (CLSM).

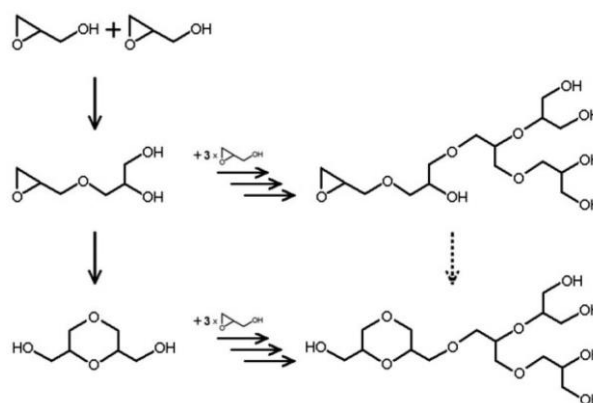
### 3 Publications and Manuscripts

#### 3.1 Estimating Kinetic Parameters for the Spontaneous Polymerization of Glycidol at Elevated Temperatures

This chapter was published in:

M. E. R. Weiss, F. Paulus, D. Steinhilber, A. N. Nikitin, R. Haag, C. Schütte, *Macromol. Theory Simul.* **2012**, *21*, 470-481;

<http://dx.doi.org/10.1002/mats.201200003>



The ring-opening polymerization of glycidol at elevated temperatures was investigated. In order to improve the synthesis of dendritic polyether polyols, experiments were performed without initiator to identify the influence of side reactions. The study revealed the influence of the thermal polymerization pathway on the dispersity of the final product and the sensitivity to the reaction temperature.

Author contribution:

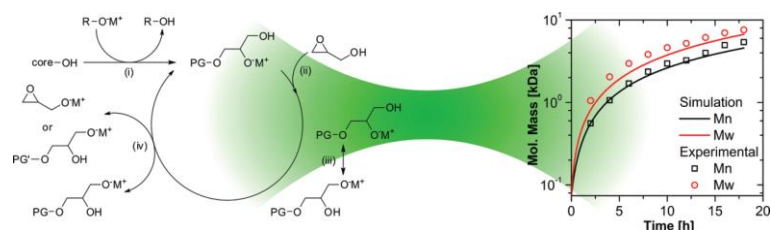
- Polyglycerol synthesis at different temperatures with sampling over 24 h
- Evaluation of GPC characterization and translation to raw data
- Support and development of the theoretical model
- Preparation of the manuscript parts: 2. Experimental section, 4.1. Experimental results
- Correction of the manuscript/page-proofs

### 3.2 Anionic Ring-Opening Polymerization Simulations for Hyperbranched Polyglycerols with Defined Molecular Weights

This chapter was published in:

F. Paulus, M. E. R. Weiss, D. Steinhilber, A. N. Nikitin, C. Schütte, R. Haag, *Macromolecules* **2013**, *46*, 8458–8466;

<http://dx.doi.org/10.1021/ma401712w>



The anionic ROMBP of dPG was investigated in detail. Different molecular weights were targeted and the reaction mixtures probed at regular intervals. The experimentally determined molecular weight distributions for each time point were subjected to extensive computer simulations to determine the rate coefficients of the base-catalyzed, thermal, inter- and intramolecular reactions. The base-catalyzed propagation was identified as the main reaction. However, the thermal propagation significantly contributed to the dynamics of the system. The thermal or base-catalyzed side reaction of self-initiation was determined to primarily increase the dispersity of the final product, especially for target molecular weights exceeding 10 000 g mol<sup>-1</sup>.

Author contribution:

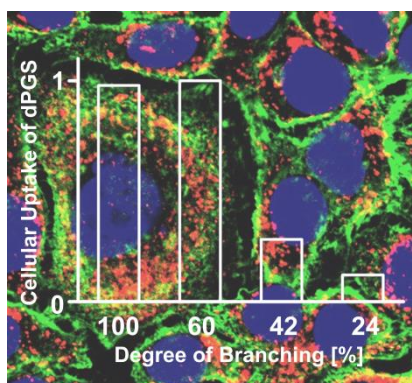
- Polyglycerol synthesis at different temperatures with sampling over 24 h
- Evaluation of GPC characterization and translation to raw data
- Preparation of the manuscript, except computer simulations

### 3.3 The Effect of Polyglycerol Sulfate Branching On Inflammatory Processes

This chapter was published in:

F. Paulus, R. Schulze, D. Steinhilber, M. Zieringer, I. Steinke, P. Welker, K. Licha, S. Wedepohl, J. Dervede, R. Haag, *Macromol. Biosci.* **2014**, *14*, 643-654;

<http://dx.doi.org/10.1002/mabi.201300420>



Different scaffold architectures of polyglycerol sulfates were synthesized and investigated for their effects on inflammatory processes and hemocompatibility. Fully glycerol-based hyperbranched polyglycerol architectures were obtained by either homopolymerization of glycidol or a new copolymerization strategy of glycidol with ethoxyethyl glycidyl ether (EEGE). Two polyglycerols with intermediate degree of branching (DB) were synthesized by using different monomer feed ratios. A perfectly branched polyglycerol dendrimer was synthesized according to an iterative two-step protocol. The biological assays showed that the DB made the different polymer conjugates perform differently with the optimal DB of 60% in all assays.

Author contribution:

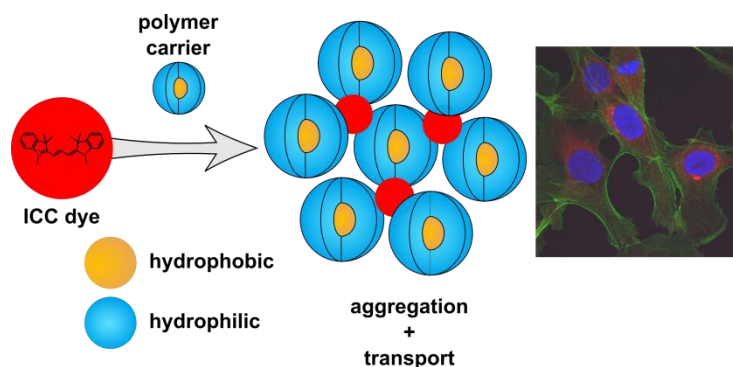
- Synthesis and purification of the EEGE monomer
- Synthesis of polyglycerols with intermediate branching
- Purification of synthesized polymers (before coupling)
- DLS and Zeta-potential measurements
- Preparation of the manuscript, except methods for competitive SPR measurements, cellular uptake studies, hemocompatibility assays

### 3.4 Structure Related Transport Properties and Cellular Uptake of Hyperbranched Polyglycerol Sulfates with Hydrophobic Cores

This chapter was published in:

F. Paulus, D. Steinhilber, P. Welker, K. Licha, D. Mangoldt, K. Licha, H. Depner, S. Sigrüst, R. Haag, *Polymer Chemistry* **2014**, *Advanced Article*;

<http://dx.doi.org/10.1039/C4PY00430B>



Different core-shell-type (CS) architectures have been investigated with respect to the encapsulation properties of hydrophobic guests. Each of three block and statistical copolymers was synthesized with different aromatic substituents and subsequently sulfated. The sulfate groups provided an electrostatic stabilization of the aggregates and a highly active targeting moiety for inflammation and cellular uptake. UV measurements show a supramolecular encapsulation of the investigated guest molecules in the low  $\mu\text{M}$  range. The transport studies with Pyrene and indocarbocyanine dye further indicated a defined core-shell-type architecture which provides a distinct amphiphilicity as required for supramolecular guest complexation. The combination of a host functionality with an active sulfate targeting moiety has been used for cellular transport.

Author contribution:

- Synthesis and purification of monomers
- Polymerization of polymer architectures, functionalization and purification
- Loading of polymer architectures with guest molecules
- DLS and UV/Vis measurements
- Preparation of the manuscript

#### 4 Summary and Conclusion

The first part of this work was focused on fundamental investigations and modeling of the ring-opening multibranching (ROMB) polymerization of dendritic polyglycerol (dPG) in solution. With a better understanding of the mechanism, the reproducibility of the process and consequently the quality of the dPG should be increased. In order to reduce the complexity of the mechanism to a smaller amount of parameters, the main and side reactions were investigated individually. Pure glycidol was polymerized at different temperatures. This thermal polymerization, which is considered a side reaction, yielded large polymeric species with high dispersities in comparison to values from classical polycondensation reactions. The main ROMB polymerization, including initiator and base-catalyst was investigated by targeting three defined molecular weights. The acquired data sets from GPC and NMR characterization were subjected to extensive computer simulations using a simplified model of the ROMB polymerization mechanism. Based on the rate coefficients determined for the thermal polymerization of glycidol, the coefficients for the base-catalyzed main reaction, the intramolecular, and the intermolecular transfer reaction were determined. The thermal propagation was identified to contribute considerably to the polymer growth.

The second part of this work focused on the structure-activity relationship of dendritic polyglycerol sulfates (dPGS) and inflammatory processes. From literature it is known that the size of the dPG scaffold and the sulfate group density on the surface influence the anti-inflammatory properties. In order to extend this knowledge with respect to the branching and flexibility of the scaffold, two dPG species with intermediate degrees of branching (DBs) were synthesized. The versatile toolbox system was manipulated by polymerization of defined monomer mixtures of glycidol and ethoxyethyl glycidyl ether (EEGE). The evaluation of the sulfated and/or dye labeled dPGS architectures was performed by cellular uptake studies with model cell lines, competitive SPR-based and blood compatibility assays. With constant molecular weight, degree of sulfation (DS), and surface charge, the conjugates performed differently, depending on the DB. Here, 60% was the ideal DB. The results presented in this work extend the knowledge of the structure-activity relationship of polyanions and especially dPGS.

The third part of this work concentrated on the synthesis of potential nanocarriers based on dPGS. As hyperbranched polymers and especially dPG are well-known scaffolds for the synthesis of unimolecular nanocarriers, the toolbox was modified and six hydrophobically derivatized core-shell-type (CS) dPGSs were synthesized. The CS-structure was varied by

using either a core-first or copolymerization approach, applying three phenyl-derivatized glycidol monomers and glycidol. Only the defined CS architectures with the hydrophobic bi-aromatic moieties exclusively located in the core were able to transport small amounts of the guest molecules Pyrene and ICC dye. The sulfated and dye-loaded architectures were able to enhance the cellular uptake of the ICC dye into model cell lines compared to the free dye. With the presented polymer architectures, it is possible to combine the unique anti-inflammatory properties of polyanions with supramolecular host properties of DDS.

## 5 Outlook

The advantages of the established model for the ROMB polymerization are enormous. With the mathematical description of the process, it is now possible to simulate variations and manipulations of the reaction conditions, e.g., monomer addition speed and its impact on the final product specification. However, it is necessary to first define the limitations of the model. This can be achieved by independent simulations of defined parameters and comparison to experimental results. The model can considerably ease further optimization in the dPG synthesis and increase the batch-to-batch reproducibility, which will serve the need for high-quality dPGs.

The discussed results on dPGS with reduced branching and the hydrophobic dPGS derivatives emphasize the versatility of the PG toolbox system and extend the knowledge of the structure-activity relationship in inflammatory processes. The change in the biological activity upon variation of the scaffold branching may be also transferred to other established conjugates to further investigate structure-activity relationships. The hydrophobic dPGS derivatives combine the good blood compatibility with supramolecular host properties of amphiphilic architectures. The presented nanocarrier systems will be further investigated for the solubilization and targeted delivery of pharmaceutically interesting molecules.



## 6 Zusammenfassung

Ziel der vorliegenden Arbeit war die Erstellung eines Modells der anionischen Ringöffnungspolymerisation von hyperverzweigten Polyglycerinen. Durch ein besseres Verständnis des zugrundeliegenden Reaktionsmechanismus kann die Reproduzierbarkeit und folglich die Produktqualität gesteigert werden. Hierbei wurde hauptsächlich der Einfluss der verschiedenen Haupt- und Nebenreaktionen hinsichtlich der resultierenden Molekulargewichtsverteilung individuell untersucht. Dadurch konnte die Komplexität des Modells in der Parametersimulation signifikant reduziert werden. Die thermische Polymerisation von Glycidol wurde bei drei verschiedenen Reaktionstemperaturen in Abwesenheit von Initiator und Basenkatalysator, durchgeführt. Über den als Nebenreaktion klassifizierten, thermischen Reaktionsweg konnten Polyglycerine mit hohen Molekulargewichten und breiter Verteilung hergestellt werden, die vergleichbar mit Werten aus den klassischen Polykondensationsreaktionen sind. Des Weiteren wurde die eigentliche Ringöffnungspolymerisation bei drei verschiedenen, definierten Molekulargewichten untersucht. Basierend auf den Daten der GPC- und NMR-Charakterisierung wurde ein vereinfachtes, computerbasiertes Modell der Polymerisation erstellt. Anhand dieses Modells konnten Reaktionskoeffizienten sowohl für die verschiedenen Reaktionswege der anionischen und thermischen Ringöffnung als auch für den intra- und intermolekularen Kationentransfer bestimmt werden. Obwohl der Koeffizient des thermischen Reaktionswegs kleiner ist als der des basenkatalysierten Hauptreaktionswegs, trägt die thermische Polymerisation signifikant zum Wachstum des Polymers bei.

In einem weiteren Teil dieser Arbeit wurde das grundlegende Verhältnis zwischen Struktur und Aktivität von Polyglycerinsulfaten in Entzündungsvorgängen untersucht. Hierbei wurde das etablierte, flexible Syntheseprotokoll modifiziert, um den Verzweigungsgrad des Polymergerüsts zu verändern. Über definierte Monomer-Mixturen/Mischungen von Glycidol und EEGE konnten Polyglycerine mit mittleren Verzweigungsgraden hergestellt werden. Die korrespondierenden Polyglycerinsulfate mit verschiedenen Verzweigungsgraden wurden hinsichtlich ihrer zellulären Aufnahme, der L-Selektin-Affinität und Blutkompatibilität charakterisiert. Hierbei zeigte sich, dass ein Verzweigungsgrad von 60% die optimale Polymer-Architektur darstellt. Die durchgeführte Studie trägt erheblich zum grundlegenden Verständnis von Entzündungsvorgängen und deren Prävention, mittels Polyglycerinsulfaten bei.

Im letzten Teil dieser Arbeit wurden vielversprechende Polyglycerinsulfat-Nanotransporter hergestellt. Es ist bekannt, dass hyperverzweigte Polymere und speziell Polyglycerine überaus geeignete Polymergerüste für Nanotransporter darstellen und mittels Copolymerisation wurden drei hydrophobe Glycidol-Derivate in die Polyglycerin-Matrix eingebaut. Hierbei wurden drei Block-Copolymere über eine 2-Stufen-Synthese und drei statistisch-verteilte Copolymere über die Polymerisation definierter Monomer-Mixturen/Mischungen hergestellt. Die Bibliothek von sechs hydrophob-derivatisierten Polyglycerinsulfaten wurde hinsichtlich der Verkapselungseigenschaften der Gastmoleküle Pyren und Indocarbocyanin charakterisiert. Es zeigte sich, dass ausschließlich die definierten Kern-Schale-Architekturen mit bi-aromatischen, hydrophoben Gruppen genügend Amphiphilie besaßen, um ein Gastmolekül zu komplexieren und transportieren. Diese Systeme waren in der Lage, die zelluläre Aufnahme im Vergleich zu dem freien Indocarbocyanin-Farbstoff zu erhöhen. Die synthetisierten, hydrophoben Polyglycerinsulfate kombinieren die einzigartigen, entzündungshemmenden Eigenschaften der Polyglycerinsulfate mit supramolekularen Trägereigenschaften.

## 7 References

- [1] a) H. Ringsdorf, *J. Polym. Sci., Polym. Sym.* **1975**, *51*, 135-153; b) R. Duncan, S. Dimitrijevic, E. G. Evagorou, *S. T. P. Pharma Sciences* **1996**, *6*, 237-263.
- [2] R. Duncan, *Nat Rev Drug Discov* **2003**, *2*, 347-360.
- [3] a) R. Haag, F. Kratz, *Angew. Chem. Int. Ed.* **2006**, *45*, 1198-1215; b) M. A. Quadir, R. Haag, *J. Control. Release* **2012**, *161*, 484-495.
- [4] a) J. Khandare, M. Calderon, N. M. Dagia, R. Haag, *Chem. Soc. Rev.* **2012**, *41*, 2824-2848; b) R. Duncan, H. Ringsdorf, R. Satchi-Fainaro, *J. Drug Target.* **2006**, *14*, 337-341.
- [5] a) R. A. Freitas, Jr., *Nanomedicine* **2005**, *1*, 2-9; b) S. Mignani, S. El Kazzouli, M. Bousmina, J.-P. Majoral, *Adv. Drug Deliver. Rev.* **2013**, *65*, 1316-1330.
- [6] a) D. S. Robinson, *Curr. Med. Res. Opin.* **1983**, *8*, 10-19; b) G. Levy, *Adv. Drug Deliver. Rev.* **1998**, *33*, 201-206; c) F. Yamashita, M. Hashida, *Adv. Drug Deliver. Rev.* **2013**, *65*, 139-147.
- [7] a) E. M. Renkin, J. P. Gilmore, *Handbook of Physiology 8: Renal Clearance*, Washington, D.C., **1973**; b) L. W. Seymour, R. Duncan, J. Strohm, J. Kopeček, *J. Biomed. Mater. Res., Part A* **1987**, *21*, 1341-1358; c) H. Soo Choi, W. Liu, P. Misra, E. Tanaka, J. P. Zimmer, B. Itty Ipe, M. G. Bawendi, J. V. Frangioni, *Nat. Biotechnol.* **2007**, *25*, 1165-1170.
- [8] R. T. Barrow, E. T. Parker, S. Krishnaswamy, P. Lollar, *J. Biol. Chem.* **1994**, *269*, 26796-26800.
- [9] a) F. M. Veronese, *Biomaterials* **2001**, *22*, 405; b) G. Pasut, F. M. Veronese, *Prog. Polym. Sci.* **2007**, *32*, 933-961; c) M. Imran ul-haq, B. F. L. Lai, R. Chapanian, J. N. Kizhakkedathu, *Biomaterials* **2012**, *33*, 9135-9147.
- [10] M. L. Immordino, F. Dosio, L. Cattel, *Int. J. Nanomed.* **2006**, *1*, 297-315.
- [11] D. Vllasaliu, R. Fowler, S. Stolnik, *Exp. Opin. Drug Deliver.* **2013**, *11*, 139-154.
- [12] S. Svenson, *Curr. Opin. Sol. State Mat. Sci.* **2012**, *16*, 287-294.
- [13] a) S. K. Hobbs, W. L. Monsky, F. Yuan, W. G. Roberts, L. Griffith, V. P. Torchilin, R. K. Jain, *Proc. Natl. Acad. Sci. U. S. A.* **1998**, *95*, 4607-4612; b) A. E. Nel, L. Madler, D. Velegol, T. Xia, E. M. V. Hoek, P. Somasundaran, F. Klaessig, V. Castranova, M. Thompson, *Nat. Mater.* **2009**, *8*, 543-557.
- [14] a) H. Maeda, J. Wu, T. Sawa, Y. Matsumura, K. Hori, *J. Control. Release* **2000**, *65*, 271-284; b) H. Maeda, *J. Control. Release* **2012**, *164*, 138-144.
- [15] a) G. Griffiths, *Nat. Rev. Mol. Cell Biol.* **2007**, *8*, 1018-1024; b) G. J. Doherty, H. T. McMahon, *Annu. Rev. Biochem.* **2009**, *78*, 857-902.
- [16] a) S. D. Conner, S. L. Schmid, *Nature* **2003**, *422*, 37-44; b) I. Canton, G. Battaglia, *Chem. Soc. Rev.* **2012**, *41*, 2718-2739.
- [17] a) M. Marsh, A. Helenius, *Cell* **2006**, *124*, 729-740; b) J. Mercer, M. Schelhaas, A. Helenius, *Annu. Rev. Biochem.* **2010**, *79*, 803-833.
- [18] a) R. Montesano, J. Roth, A. Robert, L. Orci, *Nature* **1982**, *296*, 651-653; b) H. A. Anderson, Y. Chen, L. C. Norkin, *Mol. Biol. Cell* **1996**, *7*, 1825-1834.
- [19] O. P. Perumal, R. Inapagolla, S. Kannan, R. M. Kannan, *Biomaterials* **2008**, *29*, 3469-3476.
- [20] J.-P. Behr, *Chimia* **1997**, *51*, 34-36.
- [21] V. B. Rikke, A. M. Maria, R. H. Jonas, S. M. Moghimi, L. A. Thomas, *Mol. Ther.* **2012**, *21*, 149-157.
- [22] E. Markovsky, H. Baabur-Cohen, A. Eldar-Boock, L. Omer, G. Tiram, S. Ferber, P. Ofek, D. Polyak, A. Scomparin, R. Satchi-Fainaro, *J. Control. Release* **2012**, *161*, 446-460.
- [23] N. D. Sonawane, F. C. Szoka, A. S. Verkman, *J. Biol. Chem.* **2003**, *278*, 44826-44831.

- [24] a) A. D'Emanuele, D. Attwood, *Adv. Drug Deliver. Rev.* **2005**, *57*, 2147-2162; b) S. Svenson, *Eur. J. Pharm. Biopharm.* **2009**, *71*, 445-462.
- [25] a) J. F. G. A. Jansen, E. M. M. de Brabander-van den Berg, E. W. Meijer, *Science* **1994**, *266*, 1226-1229; b) J. C. M. v. Hest, D. A. P. Delnoye, M. W. P. L. Baars, M. H. P. v. Genderen, E. W. Meijer, *Science* **1995**, *268*, 1592-1595.
- [26] a) A. Sunder, R. Mülhaupt, R. Haag, H. Frey, *Adv. Mater.* **2000**, *12*, 235-239; b) H. Frey, R. Haag, *Rev. Mol. Biotechn.* **2002**, *90*, 257-267; c) J. Khandare, A. Mohr, M. Calderón, P. Welker, K. Licha, R. Haag, *Biomaterials* **2010**, *31*, 4268-4277.
- [27] H. Türk, A. Shukla, P. C. Alves Rodrigues, H. Rehage, R. Haag, *Chem. Eur. J.* **2007**, *13*, 4187-4196.
- [28] I. N. Kurniasih, H. Liang, J. P. Rabe, R. Haag, *Macromol. Rapid Commun.* **2010**, *31*, 1516-1520.
- [29] I. N. Kurniasih, H. Liang, V. D. Moschwitz, M. A. Quadir, M. Radowski, J. P. Rabe, R. Haag, *New J. Chem.* **2012**, *36*, 371-379.
- [30] D. Steinhilber, F. Paulus, A. T. Zill, S. C. Zimmerman, R. Haag, *MRS Proceedings* **2012**, *1403*.
- [31] R. K. Kainthan, C. Mugabe, H. M. Burt, D. E. Brooks, *Biomacromolecules* **2008**, *9*, 886-895.
- [32] G. R. Newkome, C. N. Moorefield, G. R. Baker, M. J. Saunders, S. H. Grossman, *Angew. Chem. Int. Ed.* **1991**, *30*, 1178-1180.
- [33] H. Ringsdorf, B. Schlarb, J. Venzmer, *Angew. Chem. Int. Ed.* **1988**, *27*, 113-158.
- [34] S. Stevelmans, J. C. M. van Hest, J. F. G. A. Jansen, D. A. F. J. van Boxtel, E. M. M. de Brabander-van den Berg, E. W. Meijer, *J. Am. Chem. Soc.* **1996**, *118*, 7398-7399.
- [35] G. Pan, Y. Lemmouchi, E. O. Akala, O. Bakare, *J. Bioact. Compat. Polym.* **2005**, *20*, 113-128.
- [36] D. Luo, K. Haverstick, N. Belcheva, E. Han, W. M. Saltzman, *Macromolecules* **2002**, *35*, 3456-3462.
- [37] C. S. Popeney, M. C. Lukowiak, C. Böttcher, B. Schade, P. Welker, D. Mangoldt, G. Gunkel, Z. Guan, R. Haag, *ACS Macro Letters* **2012**, *1*, 564-567.
- [38] Z. Guan, P. M. Cotts, E. F. McCord, S. J. McLain, *Science* **1999**, *283*, 2059-2062.
- [39] M. R. Radowski, A. Shukla, H. v. Berlepsch, C. Böttcher, G. Pickaert, H. Rehage, R. Haag, *Angew. Chem. Int. Ed.* **2007**, *46*, 1265-1269.
- [40] a) M. A. Quadir, M. R. Radowski, F. Kratz, K. Licha, P. Hauff, R. Haag, *J. Control. Release* **2008**, *132*, 289-294; b) E. Fleige, R. Tyagi, R. Haag, in *Nanocarriers, Vol. 1*, **2013**, pp. 1-9.
- [41] a) D. D. Lasic, D. Needham, *Chem. Rev.* **1995**, *95*, 2601-2628; b) D. C. Drummond, M. Zignani, J.-C. Leroux, *Prog. Lipid Res.* **2000**, *39*, 409-460; c) D. Sutton, N. Nasongkla, E. Blanco, J. Gao, *Pharm. Res.* **2007**, *24*, 1029-1046.
- [42] E. Fleige, B. Ziem, M. Grabolle, R. Haag, U. Resch-Genger, *Macromolecules* **2012**, *45*, 9452-9459.
- [43] S. F. Haag, E. Fleige, M. Chen, A. Fahr, C. Teutloff, R. Bittl, J. Lademann, M. Schäfer-Korting, R. Haag, M. C. Meinke, *Int. J. Pharm.* **2011**, *416*, 223-228.
- [44] a) K. Kataoka, A. Harada, Y. Nagasaki, *Adv. Drug Deliver. Rev.* **2001**, *47*, 113-131; b) D. E. Discher, A. Eisenberg, *Science* **2002**, *297*, 967-973.
- [45] S. Hou, K. Y. K. Man, W. K. Chan, *Langmuir* **2003**, *19*, 2485-2490.
- [46] H.-N. Lee, Z. Bai, N. Newell, T. P. Lodge, *Macromolecules* **2010**, *43*, 9522-9528.
- [47] S. C. Kim, D. W. Kim, Y. H. Shim, J. S. Bang, H. S. Oh, S. W. Kim, M. H. Seo, *J. Control. Release* **2001**, *72*, 191-202.
- [48] S. H. Boddu, J. Jwala, M. R. Chowdhury, A. K. Mitra, *J. Ocul. Pharmacol. Ther.* **2010**, *26*, 459-468.

- [49] A. Richter, A. Wiedekind, M. Krause, T. Kissel, R. Haag, C. Olbrich, *Eur. J. Pharm. Sci.* **2010**, *40*, 48-55.
- [50] R. Tyagi, S. Malhotra, A. F. Thünemann, A. Sedighi, M. Weber, A. Schäfer, R. Haag, *J. Phys. Chem. C* **2013**, *117*, 12307-12317.
- [51] S. Gupta, B. Schade, S. Kumar, C. Böttcher, S. K. Sharma, R. Haag, *Small* **2013**, *9*, 894-904.
- [52] a) A. V. Ambade, E. N. Savariar, S. Thayumanavan, *Mol. Pharm.* **2005**, *2*, 264-272; b) C. d. I. H. Alarcon, S. Pennadam, C. Alexander, *Chem. Soc. Rev.* **2005**, *34*, 276-285; c) B. Priya, P. Viness, E. C. Yahya, C. d. T. Lisa, *Biomed. Mat.* **2009**, *4*, 022001; d) J. Kost, R. Langer, *Adv. Drug Deliver. Rev.* **2001**, *46*, 125-148; e) E. Fleige, M. A. Quadir, R. Haag, *Adv. Drug Deliver. Rev.* **2012**, *64*, 866-884.
- [53] M. Calderón, P. Welker, K. Licha, I. Fichtner, R. Graeser, R. Haag, F. Kratz, *J. Control. Release* **2011**, *151*, 295-301.
- [54] Y. Wang, S. Gao, W.-H. Ye, H. S. Yoon, Y.-Y. Yang, *Nat. Mater.* **2006**, *5*, 791-796.
- [55] a) D. Steinhilber, A. L. Sisson, D. Mangoldt, P. Welker, K. Licha, R. Haag, *Adv. Funct. Mater.* **2010**, *20*, 4133-4138; b) S. Aluri, S. M. Janib, J. A. Mackay, *Adv. Drug Deliver. Rev.* **2009**, *61*, 940-952; c) X.-M. Jiang, M. Fitzgerald, C. M. Grant, P. J. Hogg, *J. Biol. Chem.* **1999**, *274*, 2416-2423.
- [56] M. Calderón, A. Warnecke, R. Gräser, R. Haag, F. Kratz, *J. Control. Release* **2008**, *132*, e54-e55.
- [57] a) N. Nishiyama, A. Iriyama, W.-D. Jang, K. Miyata, K. Itaka, Y. Inoue, H. Takahashi, Y. Yanagi, Y. Tamaki, H. Koyama, K. Kataoka, *Nat. Mater.* **2005**, *4*, 934-941; b) G. Han, C.-C. You, B.-j. Kim, R. S. Turingan, N. S. Forbes, C. T. Martin, V. M. Rotello, *Angew. Chem. Int. Ed.* **2006**, *45*, 3165-3169.
- [58] a) G. Köhler, C. Milstein, *Nature* **1975**, *256*, 495-497; b) L. Gros, H. Ringsdorf, H. Schupp, *Angew. Chem. Int. Ed.* **1981**, *20*, 305-325.
- [59] C. Fasting, C. A. Schalley, M. Weber, O. Seitz, S. Hecht, B. Kokschi, J. Dervede, C. Graf, E.-W. Knapp, R. Haag, *Angew. Chem. Int. Ed.* **2012**, *51*, 10472-10498.
- [60] V. Kumar, S. L. Robbins, R. S. Cotran, *Robbins and Cotran pathologic basis of disease*, Elsevier, Philadelphia, Pa., **2009**.
- [61] A. K. Abbas, A. H. Lichtman, *Basic immunology functions and disorders of the immune system*, 2. ed., Saunders, Philadelphia u.a., **2004**.
- [62] W. A. Muller, *Lab. Invest.* **2002**, *82*, 521-534.
- [63] K. Ley, C. Laudanna, M. I. Cybulsky, S. Nourshargh, *Nat. Rev. Immunol.* **2007**, *7*, 678-689.
- [64] J. J. Campbell, S. Qin, K. B. Bacon, C. R. Mackay, E. C. Butcher, *J. Cell Biol.* **1996**, *134*, 255-266.
- [65] H. Ulbrich, E. E. Eriksson, L. Lindbom, *Trends Pharmacol. Sci.* **2003**, *24*, 640-647.
- [66] R. P. McEver, K. L. Moore, R. D. Cummings, *J. Biol. Chem.* **1995**, *270*, 11025-11028.
- [67] K. Ley, *Trends Mol. Med.* **2003**, *9*, 263-268.
- [68] a) U. Jung, K. Ley, *J. Immunol.* **1999**, *162*, 6755-6762; b) D. Stibenz, C. Bühner, *Scand. J. Immunol.* **1994**, *39*, 59-63.
- [69] a) E. L. Berg, L. M. McEvoy, C. Berlin, R. F. Bargatze, E. C. Butcher, *Nature* **1993**, *366*, 695-698; b) H. Kawashima, Y.-F. Li, N. Watanabe, J. Hirose, M. Hirose, M. Miyasaka, *Int. Immunol.* **1999**, *11*, 393-405.
- [70] V. Sreeramkumar, M. Leiva, A. Stadtmann, C. Pitaval, I. Ortega-Rodríguez, M. K. Wild, B. Lee, A. Zarbock, A. Hidalgo, *Blood* **2013**, *122*, 3993-4001.
- [71] B. Furie, B. C. Furie, *Trends Mol. Med.* **2004**, *10*, 171-178.

- [72] a) R. Pigott, L. A. Needham, R. M. Edwards, C. Walker, C. Power, *J. Immunol.* **1991**, *147*, 130-135; b) G. S. Kansas, K. B. Saunders, K. Ley, A. Zakrzewicz, R. M. Gibson, B. C. Furie, B. Furie, T. F. Tedder, *J. Cell Biol.* **1994**, *124*, 609-618.
- [73] a) B. J. Graves, R. L. Crowther, C. Chandran, J. M. Rumberger, S. Li, K.-S. Huang, D. H. Presky, P. C. Familletti, B. A. Wolitzky, D. K. Burns, *Nature* **1994**, *367*, 532-538; b) W. S. Somers, J. Tang, G. D. Shaw, R. T. Camphausen, *Cell* **2000**, *103*, 467-479.
- [74] W. S. Somers, J. Tang, G. D. Shaw, R. T. Camphausen, *Cell* **2000**, *103*, 467-479.
- [75] a) M. L. Phillips, E. Nudelman, F. C. A. Gaeta, M. Perez, A. K. Singhal, S.-i. Hakomori, J. C. Paulson, *Science* **1990**, *250*, 1130-1132; b) E. L. Berg, M. K. Robinson, O. Mansson, E. C. Butcher, J. L. Magnani, *J. Biol. Chem.* **1991**, *266*, 14869-14872.
- [76] E. E. Simanek, G. J. McGarvey, J. A. Jablonowski, C.-H. Wong, *Chem. Rev.* **1998**, *98*, 833-862.
- [77] M. E. Beauharnois, K. C. Lindquist, D. Marathe, P. Vanderslice, J. Xia, K. L. Matta, S. Neelamegham, *Biochemistry* **2005**, *44*, 9507-9519.
- [78] J. Egger, C. Weckerle, B. Cutting, O. Schwaradt, S. Rabbani, K. Lemme, B. Ernst, *J. Am. Chem. Soc.* **2013**, *135*, 9820-9828.
- [79] R. Stahn, H. Schäfer, F. Kernchen, J. Schreiber, *Glycobiology* **1998**, *8*, 311-319.
- [80] a) R. M. Nelson, S. Dolich, A. Aruffo, O. Cecconi, M. P. Bevilacqua, *J. Clin. Invest.* **1993**, *91*, 1157-1166; b) S. Ushiyama, T. M. Laue, K. L. Moore, H. P. Erickson, R. P. McEver, *J. Biol. Chem.* **1993**, *268*, 15229-15237.
- [81] R. E. Bruehl, F. Dasgupta, T. R. Katsumoto, J. H. Tan, C. R. Bertozzi, W. Spevak, D. J. Ahn, S. D. Rosen, J. O. Nagy, *Biochemistry* **2001**, *40*, 5964-5974.
- [82] E. L. Vodovozova, E. V. Moiseeva, G. K. Grechko, G. P. Gayenko, N. E. Nifant'ev, N. V. Bovin, J. G. Molotkovsky, *Eur. J. Cancer* **2000**, *36*, 942-949.
- [83] a) E. B. Finger, K. D. Purl, R. Alon, M. B. Lawrence, U. H. von Andrian, T. A. Springer, *Nature* **1996**, *379*, 266-269; b) M. B. Lawrence, G. S. Kansas, E. J. Kunkel, K. Ley, *J. Cell Biol.* **1997**, *136*, 717-727.
- [84] S. Enders, G. Bernhard, A. Zakrzewicz, R. Tauber, *Biochim. Biophys. Acta, Gen. Subj.* **2007**, *1770*, 1441-1449.
- [85] a) M. P. Skinner, D. J. Fournier, R. K. Andrews, J. J. Gorman, C. N. Chesterman, M. C. Berndt, *Biochem. Biophys. Res. Commun.* **1989**, *164*, 1373-1379; b) M. P. Skinner, C. M. Lucas, G. F. Burns, C. N. Chesterman, M. C. Berndt, *J. Biol. Chem.* **1991**, *266*, 5371-5374; c) B. Mulloy, M. J. Forster, *Glycobiology* **2000**, *10*, 1147-1156.
- [86] C. Mähner, M. D. Lechner, E. Nordmeier, *Carbohydr. Res.* **2001**, *331*, 203-208.
- [87] a) L. Lopalco, F. Ciccomascolo, P. Lanza, G. Zoppetti, I. Caramazza, F. Leoni, A. Beretta, A. G. Siccardi, *AIDS Res. Hum. Retrov.* **1994**, *10*, 787-793; b) T. Yoshida, H. Nakashima, N. Yamamoto, T. Uryu, *Polym. J.* **1993**, *25*, 1069-1077; c) Samtleben, Bengsch, Boos, Seide, W. Samtleben, *Artif. Organs* **1998**, *22*, 43-46; d) C. Knabbe, K. D. Voigt, EP0935000, **1991**.
- [88] J. Hirsh, T. E. Warkentin, S. G. Shaughnessy, S. S. Anand, J. L. Halperin, R. Raschke, C. Granger, E. M. Ohman, J. E. Dalen, *CHEST Journal* **2001**, *119*, 64S-94S.
- [89] M. Demir, O. Iqbal, C. P. Dietrich, D. A. Hoppensteadt, S. Ahmad, A. N. Daud, J. Fareed, *Clin. Appl. Thromb.-Hem.* **2001**, *7*, 44-52.
- [90] U. Lindahl, L. Thunberg, G. Bäckström, J. Riesenfeld, K. Nordling, I. Björk, *J. Biol. Chem.* **1984**, *259*, 12368-12376.
- [91] I. Capila, R. J. Linhardt, *Angew. Chem. Int. Ed.* **2002**, *41*, 390-412.
- [92] N. S. Gunay, R. J. Linhardt, *Planta Med.* **1999**, *65*, 301-306.

- [93] L. Wang, J. R. Brown, A. Varki, J. D. Esko, *J. Clin. Invest.* **2002**, *110*, 127-136.
- [94] J. Fritzsche, S. Alban, R. J. Ludwig, S. Rubant, W.-H. Boehncke, G. Schumacher, G. Bendas, *Biochem. Pharmacol.* **2006**, *72*, 474-485.
- [95] H. Türk, R. Haag, S. Alban, *Bioconjugate Chem.* **2004**, *15*, 162-167.
- [96] M. Mammen, S.-K. Choi, G. M. Whitesides, *Angew. Chem. Int. Ed.* **1998**, *37*, 2754-2794.
- [97] J. Dervedde, I. Papp, S. Enders, S. Wedepohl, F. Paulus, R. Haag, *J. Carbohydr. Chem.* **2011**, *30*, 347-360.
- [98] M. Weinhart, D. Gröger, S. Enders, J. Dervedde, R. Haag, *Biomacromolecules* **2011**, *12*, 2502-2511.
- [99] M. Weinhart, D. Gröger, S. Enders, S. B. Riese, J. Dervedde, R. K. Kainthan, D. E. Brooks, R. Haag, *Macromol. Biosci.* **2011**, *11*, 1088-1098.
- [100] D. A. Tomalia, J. M. J. Fréchet, in *Dendrimers and Other Dendritic Polymers*, John Wiley & Sons, Ltd, **2001**, pp. 1-44.
- [101] J. M. G. Cowie, V. Arrighi, *Polymers Chemistry and Physics of Modern Materials (3rd ed.)*, CRC Press, Boca Raton, **2008**.
- [102] D. A. Tomalia, J. B. Christensen, U. Boas, *Dendrimers, Dendrons, and Dendritic Polymers - Discovery, Applications, and the Future*, 1 ed., Cambridge University Press, Cambridge, **2012**.
- [103] R. H. Kienle, A. G. Hovey, *J. Am. Chem. Soc.* **1929**, *51*, 509-519.
- [104] R. H. Kienle, P. A. Van Der Meulen, F. E. Petke, *J. Am. Chem. Soc.* **1939**, *61*, 2258-2268.
- [105] C. Gao, D. Yan, *Prog. Polym. Sci.* **2004**, *29*, 183-275.
- [106] G. Odian, *Principles of Polymerization*, John Wiley & Sons, New York, **2004**.
- [107] a) P. J. Flory, *J. Am. Chem. Soc.* **1941**, *63*, 3091-3096; b) P. J. Flory, *J. Am. Chem. Soc.* **1941**, *63*, 3096-3100.
- [108] P. J. Flory, *J. Am. Chem. Soc.* **1952**, *74*, 2718-2723.
- [109] H. R. Kricheldorf, Q. Z. Zang, G. Schwarz, *Polymer* **1982**, *23*, 1821-1829.
- [110] Y. H. Kim, O. W. Webster, *J. Am. Chem. Soc.* **1990**, *112*, 4592-4593.
- [111] J. M. J. Fréchet, M. Henmi, I. Gitsov, S. Aoshima, M. R. Leduc, R. B. Grubbs, *Science* **1995**, *269*, 1080-1083.
- [112] a) M. Suzuki, A. Ii, T. Saegusa, *Macromolecules* **1992**, *25*, 7071-7072; b) H. Magnusson, E. Malmström, A. Hult, *Macromol. Rapid Commun.* **1999**, *20*, 453-457.
- [113] H.-T. Chang, J. M. J. Fréchet, *J. Am. Chem. Soc.* **1999**, *121*, 2313-2314.
- [114] Y. H. Kim, O. W. Webster, *Macromolecules* **1992**, *25*, 5561-5572.
- [115] F. Morgenroth, K. Müllen, *Tetrahedron* **1997**, *53*, 15349-15366.
- [116] C. J. Hawker, R. Lee, J. M. J. Fréchet, *J. Am. Chem. Soc.* **1991**, *113*, 4583-4588.
- [117] E. Malmstroem, M. Johansson, A. Hult, *Macromolecules* **1995**, *28*, 1698-1703.
- [118] L. J. Hobson, A. M. Kenwright, W. J. Feast, *Chem. Commun.* **1997**, 1877-1878.
- [119] D. H. Bolton, K. L. Wooley, *J. Polym. Sci., Part A: Polym. Chem.* **2002**, *40*, 823-835.
- [120] A. Kumar, E. W. Meijer, *Chem. Commun.* **1998**, 1629-1630.
- [121] K. E. Uhrich, C. J. Hawker, J. M. J. Fréchet, S. R. Turner, *Macromolecules* **1992**, *25*, 4583-4587.
- [122] C. J. Hawker, J. M. J. Fréchet, R. B. Grubbs, J. Dao, *J. Am. Chem. Soc.* **1995**, *117*, 10763-10764.
- [123] a) K. Matyjaszewski, J. Pyun, S. G. Gaynor, *Macromol. Rapid Commun.* **1998**, *19*, 665-670; b) V. Coessens, T. Pintauer, K. Matyjaszewski, *Prog. Polym. Sci.* **2001**, *26*, 337-377.
- [124] D. S. Zhuk, A. G. Petr, A. K. Valentin, *Russ. Chem. Rev.* **1965**, *34*, 515-527.

- [125] R. Haag, J.-F. Stumbé, A. Sunder, H. Frey, A. Hebel, *Macromolecules* **2000**, *33*, 8158-8166.
- [126] M. Liu, N. Vladimirov, J. M. J. Fréchet, *Macromolecules* **1999**, *32*, 6881-6884.
- [127] D. Turp, T.-T.-T. Nguyen, M. Baumgarten, K. Müllen, *New J. Chem.* **2012**, *36*, 282-298.
- [128] O. Boussif, F. Lezoualc'h, M. A. Zanta, M. D. Mergny, D. Scherman, B. Demeneix, J. P. Behr, *Proc. Natl. Acad. Sci. U. S. A.* **1995**, *92*, 7297-7301.
- [129] S. R. Sandler, F. R. Berg, *J. Polym. Sci., Part A: Polym. Chem.* **1966**, *4*, 1253-1259.
- [130] E. J. Vandenberg, *J. Polym. Sci., Part A: Polym. Chem.* **1985**, *23*, 915-949.
- [131] R. Tokar, P. Kubisa, S. Penczek, A. Dworak, *Macromolecules* **1994**, *27*, 320-322.
- [132] R. M. Garipov, L. R. Garipova, A. A. Efremova, *Polymer Science Series D* **2012**, *5*, 185-189.
- [133] D. Höltér, A. Burgath, H. Frey, *Acta Polym.* **1997**, *48*, 30-35.
- [134] R. Hanselmann, D. Höltér, H. Frey, *Macromolecules* **1998**, *31*, 3790-3801.
- [135] A. Sunder, R. Hanselmann, H. Frey, R. Mülhaupt, *Macromolecules* **1999**, *32*, 4240-4246.
- [136] a) M. Meise, R. Haag, *ChemSusChem* **2008**, *1*, 637-642; b) J. Keilitz, R. Haag, *Eur. J. Org. Chem.* **2009**, *2009*, 3272-3278; c) V. S. Thengarai, J. Keilitz, R. Haag, *Inorg. Chim. Acta* **2014**, *409*, Part A, 179-184.
- [137] a) M. Hu, M. Chen, G. Li, Y. Pang, D. Wang, J. Wu, F. Qiu, X. Zhu, J. Sun, *Biomacromolecules* **2012**, *13*, 3552-3561; b) R. A. Sheno, B. F. L. Lai, J. N. Kizhakkedathu, *Biomacromolecules* **2012**, *13*, 3018-3030; c) D. Steinhilber, M. Witting, X. Zhang, M. Staegemann, F. Paulus, W. Friess, S. Küchler, R. Haag, *J. Control. Release* **2013**, *169*, 289-295.
- [138] a) S. Reichert, P. Welker, M. Calderón, J. Khandare, D. Mangoldt, K. Licha, R. K. Kainthan, D. E. Brooks, R. Haag, *Small* **2011**, *7*, 820-829; b) S. Biffi, S. Dal Monego, C. Dullin, C. Garrovo, B. Bosnjak, K. Licha, P. Welker, M. M. Epstein, F. Alves, *PLoS One* **2013**, *8*, 1-9; c) J. Dervede, A. Rausch, M. Weinhart, S. Enders, R. Tauber, K. Licha, M. Schirner, U. Zügel, A. von Bonin, R. Haag, *Proc. Natl. Acad. Sci. U. S. A.* **2010**, *107*, 19679-19684.
- [139] A. Burgath, A. Sunder, H. Frey, *Macromol. Chem. Phys.* **2000**, *201*, 782-791.
- [140] M. Calderón, M. A. Quadir, S. K. Sharma, R. Haag, *Adv. Mater.* **2010**, *22*, 190-218.
- [141] D. Wilms, F. Wurm, J. Nieberle, P. Böhm, U. Kemmer-Jonas, H. Frey, *Macromolecules* **2009**, *42*, 3230-3236.
- [142] R. K. Kainthan, E. B. Muliawan, S. G. Hatzikiriakos, D. E. Brooks, *Macromolecules* **2006**, *39*, 7708-7717.
- [143] M. Imran ul-haq, R. A. Sheno, D. E. Brooks, J. N. Kizhakkedathu, *J. Polym. Sci., Part A: Polym. Chem.* **2013**, *51*, 2614-2621.
- [144] X. Yu, Z. Liu, J. Janzen, I. Chafeeva, S. Horte, W. Chen, R. K. Kainthan, J. N. Kizhakkedathu, D. E. Brooks, *Nat. Mater.* **2012**, *11*, 468-476.
- [145] I. Vroman, L. Tighzert, *Materials* **2009**, *2*, 307-344.
- [146] a) D. Steinhilber, S. Seiffert, J. A. Heyman, F. Paulus, D. A. Weitz, R. Haag, *Biomaterials* **2011**, *32*, 1311-1316; b) H. Zhou, D. Steinhilber, H. Schlaad, A. L. Sisson, R. Haag, *React. Funct. Polym.* **2011**, *71*, 356-361.
- [147] J. C. Cuggino, C. I. Alvarez I, M. C. Strumia, P. Welker, K. Licha, D. Steinhilber, R.-C. Mutihac, M. Calderon, *Soft Matter* **2011**, *7*, 11259-11266.
- [148] W. H. Carothers, *Trans. Farad. Soc.* **1936**, *32*, 39-49.
- [149] P. J. Flory, *Principles of Polymer Chemistry*, Cornell Univ. Press, Ithaca, New York, **1953**.



- [150] a) G. Moad, D. H. Solomon, in *The Chemistry of Radical Polymerization (Second Edition)* (Eds.: G. Moad, D. H. Solomon), Elsevier Science Ltd, Amsterdam, **2005**, pp. 413-449; b) G. Moad, D. H. Solomon, in *The Chemistry of Radical Polymerization (Second Edition)* (Eds.: G. Moad, D. H. Solomon), Elsevier Science Ltd, Amsterdam, **2005**, pp. 451-585.
- [151] A. Sunder, H. Frey, R. Mülhaupt, *Macromol. Symp.* **2000**, *153*, 187-196.
- [152] a) J. Chiefari, J. Jeffery, R. T. A. Mayadunne, G. Moad, E. Rizzardo, S. H. Thang, *Macromolecules* **1999**, *32*, 7700-7702; b) A.-M. Zorn, M. Malkoch, A. Carlmark, C. Barner-Kowollik, *Polym. Chem.* **2011**, *2*, 1163-1173.

## 8 Patent Applications, Publications and Conference Contributions

### 8.1 Patent Applications

- 1) Rainer Haag, **Florian Paulus**, *Dendritische Polyglycerolsulfate dPGS-Effektorkonjugate*. Europäische Patentanmeldung **2010**, EP 100 021 21.1.
- 2) Kai Licha, Michael Schirner, Pia Welker, Rainer Haag, Marie Weinhart, **Florian Paulus**, *Polyanionic multivalent macromolecules for intracellular targeting of proliferation and protein synthesis*. PCT Int. Appl. **2011**, 98 pp. WO 2011095311.
- 3) Rainer Haag, **Florian Paulus**, *Verfahren zur Herstellung Polyglycerin-basierter Kern-Schale-Polymere mit hydrophoben Gruppen sowie anionischer Funktionalisierung, zum Einsatz als unimolekulare Nanotransporter für Wirk- und Farbstoffe zur zellulären Aufnahme*. Deutsche Patentanmeldung **2014**.

### 8.2 Publications

- 1) Jens Dervedde, Ilona Papp, Sven Enders, Stefanie Wedepohl, **Florian Paulus**, Rainer Haag; *Synthesis and Evaluation of Nonsulfated and Sulfated Glycopolymers as L- and P-selectin Inhibitors*, Journal of Carbohydrate Chemistry **2011**, 30, 347-360.
- 2) Dirk Steinhilber, Sebastian Seiffert, John A. Heyman, Florian Paulus, David A. Weitz, Rainer Haag; *Hyperbranched polyglycerols on the nanometer and micrometer scale*, Biomaterials **2011**, 32, 1311-1316.
- 3) Dirk Steinhilber, **Florian Paulus**, Andrew T. Zill, Steven C. Zimmerman, Rainer Haag; *Calix[8]arene Functionalized Polyglycerol Nanogels for Encapsulation and Stabilization of Fluorescent Dyes*, MRS Proceedings **2012**, 1403 pp.
- 4) Maximilian E. R. Weiss, **Florian Paulus**, Dirk Steinhilber, Anatoly N. Nikitin, Rainer Haag, Christof Schütte; *Estimating Kinetic Parameters for the Spontaneous Polymerization of Glycidol at Elevated Temperatures*, Macromolecular Theory and Simulations **2012**, 21, 470-481.
- 5) Dirk Steinhilber, Madeleine Witting, Xuejiao Zhang, Michael Staegemann, **Florian Paulus**, Wolfgang Friess, Sarah Küchler, Rainer Haag; *Surfactant free preparation of biodegradable dendritic polyglycerol nanogels by inverse nanoprecipitation for encapsulation and release of pharmaceutical biomacromolecules*, Journal of Controlled Release **2013**, 169, 289-295.
- 6) Dominic Gröger, **Florian Paulus**, Kai Licha, Pia Welker, Marie Weinhart, Cornelia Holzhausen, Lars Mundhenk, Achim D. Gruber, Ulrich Abram, Rainer

- Haag; *Synthesis and Biological Evaluation of Radio and Dye Labeled Amino Functionalized Dendritic Polyglycerol Sulfates as Multivalent Anti-Inflammatory Compounds*, *Bioconjugate Chemistry* **2013**, *24*, 1507-1514.
- 7) **Florian Paulus**, Maximilian E. R. Weiss, Dirk Steinhilber, Anatoly N. Nikitin, Christof Schütte, Rainer Haag; *Anionic Ring-Opening Polymerization Simulations for Hyperbranched Polyglycerols with Defined Molecular Weights*, *Macromolecules* **2013**, *46*, 8458-8466.
- 8) Dirk Steinhilber, Torsten Rossow, Stefanie Wedepohl, **Florian Paulus**, Sebastian Seiffert, Rainer Haag; *A Microgel Construction Kit for Bioorthogonal Encapsulation and pH-Controlled Release of Living Cells*, *Angewandte Chemie International Edition* **2013**, *52*, 13538-13543.
- 9) **Florian Paulus**, Ronny Schulze, Dirk Steinhilber, Maximilian Zieringer, Ingo Steinke, Pia Welker, Kai Licha, Stefanie Wedepohl, Jens Dervede, Rainer Haag; *The Effect of Polyglycerol Sulfate Branching On Inflammatory Processes*, *Macromolecular Bioscience* **2014**, *14*, 643-654.
- 10) **Florian Paulus**, Dirk Steinhilber, Pia Welker, Kai Licha, Helmut Schlaad, Rainer Haag; *Structure Related Transport Properties and Cellular Uptake of Hyperbranched Polyglycerol Sulfates with Hydrophobic Cores*, *Polymer Chemistry* **2014**, *Advanced Article*, DOI: 10.1039/C4PY00430B.
- 11) Pradip Dey, Miriam Adamovoski, Simon Friebe, Artavazd Badalyan, Radu-Cristian Mutihac, **Florian Paulus**, Silke Leimkühler, Ulla Wollenberger, Rainer Haag; *Dendritic Polyglycerol-polyethylene glycol based polymer networks for biosensing applications*, *ACS Applied Materials & Interfaces* **2014**, *Article ASAP*, DOI: 10.1021/am502018x.

### 8.3 Conference Contributions

#### Poster Presentations

- 1) Polymers in Biomedicine and Electronics – Biannual Meeting of the GDCh-Division Macromolecular Chemistry and Polydays, Berlin, Germany (3-5 October 2010); Poster: Batch Reactor Synthesis of Functionalized Hyperbranched Polyglycerol Sulfates: A Novel One-Pot Procedure; **Florian Paulus**, Dirk Steinhilber, Sylvia Kern, Nicole Wegner, Kai Licha, Rainer Haag.
- 2) 8<sup>th</sup> International Symposium on Polymer Therapeutics: From Laboratory to Clinical Practice, Valencia, Spain (24-26 May 2010); Poster: Batch Reactor Synthesis of Functionalized Hyperbranched Polyglycerol Sulfates: A Novel One-Pot Procedure;

**Florian Paulus**, *Dirk Steinhilber, Sylvia Kern, Nicole Wegner, Kai Licha, Rainer Haag.*

- 3) SFB765 Graduate School – 2<sup>nd</sup> external Doctoral Student’s workshop, Rheinsberg, Germany (21-23 September 2011); Poster: Batch Reactor Synthesis of Functionalized Hyperbranched Polyglycerol Sulfates: A Novel One-Pot Procedure; **Florian Paulus**, *Dirk Steinhilber, Sylvia Kern, Nicole Wegner, Kai Licha, Rainer Haag.*
- 4) 27. TDC - Tag der Chemie, Berlin, Germany (28. June 2012); Poster: Dendritic Polyglycerol Sulfate (dPGS) in Inflammatory Settings: Upscaling and Selectin Inhibition Structure-Activity Relationship; **Florian Paulus**, *Dominic Gröger, Rainer Haag.*
- 5) 125<sup>th</sup> BASF International Summer Course, Ludwigshafen, Germany (30 July – 8 August 2013); Poster: Biological Properties of Anti-Inflammatory Polyglycerol Sulfates – Branching Matters; **Florian Paulus**, *Ronny Schulze, Dirk Steinhilber, Maximilian Zieringer, Ingo Steinke, Pia Welker, Stefanie Wedepohl, Kai Licha, Jens Dervedde, Rainer Haag.*

#### **Oral Presentations**

- 1) 1<sup>st</sup> combined external doctoral students workshop – Graduate Schools SFBs 765 and 858, Rheinsberg, Germany (6-8 March 2013); Oral presentation: L-selectin Inhibition & Cellular Uptake of dPGS with Different Degrees of Branching; **Florian Paulus**, *Rainer Haag.*

## **9 Curriculum Vitae**

Der Lebenslauf ist in der Online-Version aus Gründen des Datenschutzes nicht enthalten.



